Since January 2020 Elsevier has created a COVID-19 resource centre with free information in English and Mandarin on the novel coronavirus COVID-19. The COVID-19 resource centre is hosted on Elsevier Connect, the company's public news and information website.

Biomaterials 238 (2020) 119828

Contents lists available at ScienceDirect

Biomaterials

journal homepage: www.elsevier.com/locate/biomaterials

Magnesium and vitamin C supplementation attenuates steroid-associated osteonecrosis in a rat model

Li-Zhen Zheng[a], Jia-Li Wang[f,a], Jian-Kun Xu[a], Xiao-Tian Zhang[d], Bao-Yi Liu[e], Le Huang[a], Ri Zhang[a], Hai-Yue Zu[a], Xuan He[a], Jie Mi[a], Qian-Qian Pang[a], Xin-Luan Wang[c], Ye-Chun Ruan[d], De-Wei Zhao[e,**], Ling Qin[a,b,c,*]

[a] Musculoskeletal Research Laboratory, Department of Orthopaedics & Traumatology, The Chinese University of Hong Kong, Hong Kong, China
[b] Innovative Orthopaedic Biomaterial and Drug Translational Research Laboratory, Li Ka Shing Institute of Health Sciences, The Chinese University of Hong Kong, Shatin, Hong Kong, China
[c] Translational Medicine R&D Center, Institute of Biomedical and Health Engineering, Shenzhen Institutes of Advanced Technology, Chinese Academy of Sciences, Shenzhen, China
[d] Department of Biomedical Engineering, Faculty of Engineering, The Hong Kong Polytechnic University, Hong Kong, China
[e] Department of Orthopaedic Surgery, Affiliated Zhongshan Hospital of Dalian University, Dalian, Liaoning Province, China
[f] School of Biomedical Engineering, Sun Yat-sen University, Guangzhou, China

ARTICLE INFO

Keywords:
Corticosteroids
Osteonecrosis
Magnesium
Vitamin C
Preclinical studies

ABSTRACT

Magnesium (Mg)-based biometal attracts clinical applications due to its biodegradability and beneficial biological effects on tissue regeneration, especially in orthopaedics, yet the underlying anabolic mechanisms in relevant clinical disorders are lacking. The present study investigated the effect of magnesium (Mg) and vitamin C (VC) supplementation for preventing steroid-associated osteonecrosis (SAON) in a rat experimental model. In SAON rats, 50 mg/kg Mg, or 100 mg/kg VC, or combination, or water control was orally supplemented daily for 2 or 6 weeks respectively. Osteonecrosis was evaluated by histology. Serum Mg, VC, and bone turnover markers were measured. Microfil-perfused samples prepared for angiography and trabecular architecture were evaluated by micro-CT. Primary bone marrow cells were isolated from each group to evaluate their potentials in osteoblastogenesis and osteoclastogenesis. The mechanisms were tested *in vitro*. Histological evaluation showed SAON lesions in steroid treated groups. Mg and VC supplementation synergistically reduced the apoptosis of osteocytes and osteoclast number, and increased osteoblast surface. VC supplementation significantly increased the bone formation marker PINP, and the combination significantly decreased the bone resorption marker CTX. TNFα expression and oxidative injury were decreased in bone marrow in Mg/VC/combination group. Mg significantly increased the blood perfusion in proximal tibia and decreased the leakage particles in distal tibia 2 weeks after SAON induction. VC significantly elevated the osteoblast differentiation potential of marrow cells and improved the trabecular architecture. The combination supplementation significantly inhibited osteoclast differentiation potential of marrow cells. *In vitro* study showed promoting osteoblast differentiation effect of VC, and anti-inflammation and promoting angiogenesis effect of Mg with underlying mechanisms. Mg and VC supplementation could synergistically alleviate SAON in rats, indicating great translational potentials of metallic minerals for preventing SAON.

1. Introduction

Stainless steel and titanium are current metals used as bioinert and permeant Class-III implants for orthopaedic applications. Recently, bioactive or biodegradable metals have attracted great attention in research and development (R&D) of biomaterials for clinical applications [1–4]. Our recent clinical work showed that the bone grafting fixation using biodegradable pure Mg screw was beneficial for successful fixation of bony flap used for treatment of osteonecrosis of the femoral head (ONFH) in patients with steroid-associated osteonecrosis

* Corresponding author. Rm74026, 5/F, Clinical Science Building, Prince of Wales Hospital, Shatin, Hong Kong Special Administrative Region.
** Corresponding author (responsible for clinical data issues). Department of Orthopaedic Surgery, Affiliated Zhongshan Hospital of Dalian University, No. 6 Jiefang Street, Dalian, 116001, Liaoning, China.
E-mail addresses: zhaodewei2000@163.com (D.-W. Zhao), lingqin@cuhk.edu.hk (L. Qin).

https://doi.org/10.1016/j.biomaterials.2020.119828
Received 4 October 2019; Received in revised form 7 January 2020; Accepted 25 January 2020
Available online 31 January 2020
0142-9612/

(SAON) where bony flap displacement was avoided and local bone density was increased accompanied by Mg-screw degradation, partially explained by the biologic effects of degraded Mg ions, yet like many available related clinical studies the scientific or mechanistic evidence was lacking [5].

SAON is a common orthopaedic disease occurring after pulsed/long term corticosteroids (CS) treatment for infectious diseases (such as severe acute respiratory syndrome, SARS) and rheumatoid diseases (such as rheumatoid arthritis, systemic lupus erythematosus, SLE) [6–8]. The occurrence of SAON is highly associated with the dosage and duration usage of CS. The incidence of ONFH was 0.7%–33% with CS treatment [9]. High dose of CS treatment for SLE even induced 44% SAON in the hips and knees [10]. Osteonecrosis (ON) may subsequently progress to joint collapse and eventually require total joint replacement [6,11]. So, it is highly desirable to study the pathogenesis of SAON and potential biomaterials established to attenuate SAON and promote the repair of SAON in early stage to prevent SAON induced joint collapse.

Excess CS treatment could directly increase apoptosis of osteoblasts and osteocytes [12], decrease the activity and differentiation of osteoblast [13], impair fat metabolism [14] and angiogenesis that induces ischemia and eventually lead to SAON [15]. Clinical evidences suggested that excess CS treatment in patients could induce lower serum magnesium (Mg) [16]. Animal models and human studies revealed that Mg deficiency was associated with osteoporosis [17], lipid metabolism [18] and vascular damage [19], which are correlated with the mechanisms of SAON. So, we hypothesized that Mg supplementation might alleviate Mg deficiency induced bone deterioration, disordered lipid metabolism and vascular damage and then attenuate SAON.

Besides, oxidative stress is also a high risk in SAON [20]. In a rabbit model, oxidative injury was present in bone marrow shortly after CS administration and before the development of SAON [21]. It was reported that the antioxidative substance vitamin E could prevent SAON due to its antioxidant property [22]. Vitamin C (VC) is a more portent antioxidant than vitamin E that VC also has benefit effect on bone development and maintenance by promoting genes producing bone matrix in osteoblasts [23]. VC supplementation may therefore attenuate SAON and promote the repair of SAON through its antioxidative effect and bone-anabolic effect.

Based on the multi-factors in the pathogenesis of SAON, combination treatment may be better than single treatment. Indeed, it was reported that combined use of an anticoagulant and a lipid-lowering agent prevented SAON more significantly than single use [24]. We hypothesized that combination of Mg and VC treatment might exert better effect than single Mg or VC treatment. The established SAON rat model was used in this study [25].

2. Materials and methods

2.1. Clinical serum Mg data collection

The clinical serum Mg data for the study of osteonecrosis (ON) was approved by the Human Ethics Committee of the Affiliated Zhongshan Hospital of Dalian University, Dalian, China. The clinical serum Mg data were collected from 35 ON patients: 18 SAON patients with CS used before, 7 SAON patients being treated with CS and 10 other ON patents. All patients gave informed consent to participate before data collection.

2.2. Study I. In vitro study

2.2.1. Culture of cell lines

MC3T3-E1 murine pre-osteoblast cell line (Subclone 14, CRL-259, ATCC, Manassas, VA, United States) was cultured in ascorbic acid free α-MEM (A10490, Gibco™, Thermo Fisher Scientific) containing 10% FBS, 1% PSN at 37 °C in a humidified atmosphere with 5% CO_2.

RAW264.7 murine macrophages (TIB-71, ATCC) were cultured in ascorbic acid free α-MEM (A10490, Gibco™, Thermo Fisher Scientific) containing 10% FBS, 1% PSN at 37 °C in a humidified atmosphere with 5% CO_2.

The human umbilical vein cell line EA.hy926 (CRL-2922™, ATCC) was cultured in Dulbecco's Modified Eagle's Medium (DMEM) without Calcium(Ca)/Mg (SH30262.01, HYCLONE, USA) with 1.8 mM $CaCl_2$ and 0.8 mM $MgCl_2$ added and containing 10% FBS, 1% PSN at 37 °C in a humidified atmosphere with 5% CO_2.

Human umbilical vein endothelial cells (HUVEC, ATCC Number: PCS-100-013, VA, USA) were cultured in ECM medium containing 5% FBS, ECGS, 100 U/ml of penicillin and streptomycin (ScienCellResearch Laboratories San Diego, California, USA) at 37 °C in a 5% CO_2. HUVECs were passaged by using 0.25% trypsin, and passages 5–6 were used in all experiments. The medium was changed every other day until the cells became confluent.

2.2.2. Cell viability assay

Tetrazolium (MTT) method and Live/Dead staining were performed to evaluate the effect of Mg and VC on the viability of MC3T3-E1 cells. For MTT test, the cells were seeded onto 96-well plates at a density of 2×10^3 cells/well. After overnight incubation, the cells were treated with different concentrations of methylprednisolone (MPS) or lipopolysaccharide (LPS) with/without Mg and VC supplemented for 24 h. Then cells were incubated with 50 μl (1 mg/ml) MTT solution at 37 °C in dark for 4 h. After discarding the MTT solution, 50 μl DMSO was added to each well, and the absorbance at 575 nm was detected. For Live/Dead staining, the cells were seeded onto 4-well chamber slides at a density of 1×10^4 cells/well. After overnight incubation, the cells were treated with different concentrations of MPS with/without Mg and VC supplemented for 24 h. Then cells were stained with live/dead cell imaging kit (488/570) (R37601, Invitrogen) and analyzed under a fluorescence microscope (Leica DM5500; Leica Micro-systems, Wetzlar, Germany).

2.2.3. In vitro osteoblast differentiation

At confluence, MC3T3-E1 were treated with/without 50 mg/L vitamin C, 10 mM of β-glycerophosphate, 100 ng/ml LPS, 1 μM of MPS, and different concentration of Mg ion. Alkaline phosphatase (ALP) activity was measured using ALP assay Kit (Biosystems, Barcelona, Spain), normalized by total protein concentrations of cell lysates which were determined biochemically using the Bradford protein assay kit (BioRad, USA). Cell mineralization was investigated by calcium nodules staining using alizarin red S.

2.2.4. In vitro osteoclastogenesis assay

To induce osteoclasts, RAW264.7 cells (5000 cells/cm^2) were cultured in the presence of receptor activator of nuclear factor kappa-B ligand (RANKL, 20 ng/ml), Mg (0 or 10 mM) and VC (0 or 50 μg/ml) for 4 days. Then quantitative real-time PCR (qRT-PCR) analysis and tartrate-resistant acid phosphatase (TRAP) staining (cat# 387, sigma) were conducted. TRAP-positive multinucleated cells with more than three nuclei were counted as osteoclasts under a light microscope. To further study the Mg effect on osteoclastogenesis induced by LPS or RANKL, RAW264.7 cells (5000 cells/cm^2) were cultured with LPS (100 ng/ml) or RANKL (20 ng/ml) plus Mg (0 or 10 mM) for 4 days for TRAP staining and qRT-PCR, and for 6 days for bone resorption function testing with the medium changed every 3 days. Osteo Assay Surface 24-well Multiple Well Plate (Corning, Product Number 3987) was used for testing the resorption function with pit formation assay. After cell culture for 6 days, the cells on the plate were lysed by 4% NaClO and the plate was washed with deionized water. The pit area in each plate was imaged (Leica DM5500; Leica Micro-systems, Wetzlar, Germany) and analyzed by ImageJ (version 1.51, Wayne Rasband, National Institute of Heath, USA).

2.2.5. Western blot (WB) analysis for cytoplasmic and nuclear proteins expression

RAW264.7 cells were grown in 100 mm dish to 50% confluency and then treated with LPS (100 ng/ml) or RANKL (20 ng/ml) with or without Mg (10 mM). After 30 min treatment, the cytoplasmic and nuclear proteins were extracted using Nuclear Extraction Kit (ab221978, abcam). The protein concentrations of cytosol and nuclear fractions were determined by Pierce™ BCA Protein Assay Kit (Catalog number: 23227, Thermo Scientific). 10 μg/lane proteins were electrophoresed on SDS-PAGE gels and transferred to nitrocellulose membranes. Then the membranes were blocked with 5% BSA in tris-buffered saline with Tween 20 (TBST) for 2 h and incubated with primary antibody overnight at 4 °C. The membranes were washed with TBST and incubated with horseradish peroxidase (HRP)-conjugated secondary antibody for 1 h at room temperature and then washed with TBST. Then the primary antibody binding was visualized using Pierce™ ECL Western Blotting Substrate (Catalog number: 32106, Thermo Scientific) and quantified with ImageJ (version 1.51, Wayne Rasband, National Institute of Heath, USA).

2.2.6. Fluorescence imaging of intracellular calcium (Ca) ions

Intracellular Ca ions images were acquired using fluorescent microscopy [26]. RAW264.7 cells were grown on 25 mm diameter glass coverslips at a density of $1 \times 10^4/cm^2$ 24 h before testing. After washed three times with Mg free Margo solution (130 mM NaCl, 5 mM KCl, 2.5 mM $CaCl_2$, 20 mM HEPES (N-2-hydroxyethylpiperazine-N′-2-ethanesulphonic acid) and 10 mM glucose, pH = 7.4), the cells were incubated in the Margo solution with 2 μM Ca-Fura-2 (Molecular Probe, Invitrogen, California, USA) and 1 μM Pluronic F-127 (Life Technologies, USA) for 30 min at 37 °C in a humidified atmosphere to load the Ca^{2+} probe. After washed three times with Margo solution and kept at 37 °C in the dark for another 30 min in Margo solution, the cells were ready for imaging. LPS (100 ng/ml), RANKL (50 ng/ml) and $MgCl_2$ (10 mM) were separately added to cell chamber for acquisition the intensity of intracellular fluorescence over time. Ca^{2+} free solution was used as control to find if intracellular Ca^{2+} changes with extracellular LPS or RANKL treatment. NMDG (*N*-methyl-D-glucamine) chloride (NMDG-Cl) was used as chloride control because we use $MgCl_2$ as the Mg source. Fluorescence with a dual excitation at 340 and 380 nm for emission collection at 510 nm was captured using the fluorescence microscope (Nikon Eclipse Ti, Japan) equipped with a CCD camera (Spot Xplorer, USA) and a Fluor 20× objective lens (0.75 NA, Nikon, Japan). Fluorescence intensity at 340 nm reflects intracellular Ca^{2+} probes combined with Ca ion, and intensity at 380 nm reflects the intracellular free Ca^{2+} probes. ΔF/F0 was used to present the change of fluorescence intensity ratio. ΔF equals the maximal fluorescence intensity ratio subtract the initial fluorescence intensity ratio and F0 equals the initial fluorescence intensity ratio.

2.2.7. In vitro angiogenesis assay

Migration of EA.hy926 was tested by scratch-wound healing assay. When cells became confluent monolayer, a denuded area was created. Then cells were treated with different concentrations of Mg ions. Mg free medium with normal calcium (1.8 mM) was used as control. Images of the denuded area were taken at time zero and 6 h later. The migration is calculated by the travel rate of EA.hy926 [27].

Tube formation of EA.hy926 was performed using Matrigel Basement Membrane Matrix (#354234, Corning). Cells starved in serum free medium overnight and throughout the rest of the experiment. Matrigel was 1:1 diluted with serum free medium and 200 μl Matrigel mixture was coated into each well of 24 well plates. The plate was put in 37 °C incubator for 30 min for gelation. Cell suspension (with 7×10^4 cells in 200 μl) was seeded onto each well coated with Matrigel. Matrigel cultures were incubated at 37 °C for 6 h. Tube formation was imaged using an inverted phase contrast microscope and analyzed by ImageJ with the Angiogenesis Analyzer plugin [28].

2.2.8. Endothelial cell permeability assay

The permeability of *in vitro* blood vessel monolayer was determined by using Transwell (12 mm in diameter, 0.4 μm pore polycarbonate membrane, Corning Inc., Corning, NJ) and Fluorescein isothiocyanate (FITC)-labeled dextran (70 kDa, Invitrogen) [29]. HUVECs were seeded in the upper chamber for 3 days to establish monolayer. The upper and lower chambers were replaced with serum free medium for 2 h. Then LPS (100 ng/ml)/Mg (10 mM) was added in the upper chamber for 4 h. Then the medium of upper chamber was replaced with 500 μl FITC–-Dextran (1 mg/ml). The lower chamber containing 1500 μl serum free medium was collected 30 min later. The fluorescence intensity of each sample was determined by a multi-label reader (VICTOR X4, PerkinElmer) at 485/535 nm.

2.2.9. Immunofluorescence (IF) staining

To study the endothelia cell monolayer, cobblestone pattern of the tight junction, zonula occludens (ZO-1) was stained with *anti*-ZO-1 (ZO1-1A12, Invitrogen) conjugated with Alexa Fluor 488, #339188). The localization of NF-kB was stained with the *anti*–NF–kB p65 antibody (ab16502, abcam).

2.3. Study II. In vivo study

2.3.1. Experimental animals, grouping and treatment

The experimental protocols (Ref No. 17-087-MIS) was reviewed and approved by Animal Experimental Ethics Committee of the Chinese University of Hong Kong. Both the *Guide for the Care and Use of Laboratory Animal* (1996) [30] and the ARRIVE (Animals in Research: Reporting *In Vivo* Experiments) guidelines [31] were followed.

Eighty 24-week-old male Sprague-Dawley rats (body weight 500–550 g) were housed in a temperature-controlled room (25 °C) under a 12/12 h reversed day/night cycle and received food and water *ad libitum*.

Sixty-four Rats were used to induce steroid-associated osteonecrosis (SAON) with sequential injections of lipopolysaccharide (LPS) and methylprednisolone (MPS) [25]. At day 1, under anesthesia with 90 mg/kg ketamine and 10 mg/kg xylazine (i.p.), the rats were intravenously injected with 0.2 mg/kg LPS (*Escherichia coli* O111:B4; Sigma-Aldrich, St. Louis, MO, USA) via tail vein steadily with slow rate (the injection time was over 30 min). From day 2, rats were intraperitoneally injected three injections of 100 mg/kg MPS (Pfizer Manufacturing Belgium NV) for three continuous days. From week 2, intraperitoneally injections of 40 mg/kg MPS were given three times a week until sacrificed by injecting overdose of pentobarbital.

The SAON induced rats were randomly divided into four groups: Mg supplementation group (Mg group), VC supplementation group (VC group), Combination supplementation group (Mg + VC group) and control group (SAON group). From the first day of MPS injection, Mg sulfate (Sigma-Aldrich) solution (providing 50 mg/kg/day Mg ion), sodium ascorbate (Sigma-Aldrich) solution (providing 100 mg/kg/day vitamin C) and combine solution (providing 50 mg/kg/day Mg ion and 100 mg/kg/day vitamin C) were prepared daily with fresh drinking water and orally administrated to the rats. The dosages were calculated based on clinical trials on Mg supplementation in diseases with Mg deficiency: about 500 mg/day [32,33], and the recommended VC dosage 1000 mg/day for treatment of clinical diseases [34]. For the SAON control group, drinking water without supplementation were orally administrated. Sixteen rats without treatment were used as normal controls (n = 8/time point). At 2 and 6 weeks after induction, before sacrificed, serum was collected. Micro-fil perfusion was performed for angiography. Bilateral femora and bilateral tibiae were collected for micro-CT and histological examinations.

2.3.2. Micro-CT based angiography

Perfusion: Under anesthesia with i.v. injection of 2.5% pentobarbital, the abdomen cavity of the rat was opened and abdominal

aorta was exposed for perfusion with Microfil® (MV-122, Flow Tech; Carver, MA, USA) using established protocol (n = 4/group) [35–37]. Then the rats were sacrificed and stored at 4 ˚C overnight to allow complete polymerization of the perfused Microfil.

Micro-angiography: After fully decalcification with 10% EDTA (pH7.4), the tibiae were scanned using a μCT-40 (Scanco Medical, Brüttisellen, Switzerland) imaging system. For proximal tibia, a 3 mm thick, 3 mm in diameter and 2 mm apart from the growth plate cylinder was used as ROI; and for distal tibia, the 3 mm thick whole bone marrow region from distal end was used as ROI. The Gaussian filter with Sigma = 1.2, Support = 2 and threshold = 120 HU was used to reconstruct 3D angiographic architecture [38]. A histogram was generated to display the thickness of the perfused Microfil [36,38].

2.3.3. Micro-CT based trabecular architecture

To determine the trabecular architecture, the tibiae from each group (at week 6) were fixed in buffered formalin and then scanned using a μCT-40 (Scanco Medical, Brüttisellen, Switzerland) imaging system. The trabecular bone with thickness of 2 mm and 2 mm from the growth plate was used as ROI. The spatial resolution is 15 μm. A low-pass Gaussian filter Sigma = 0.8, Support = 1, and threshold = 220 HU was used to reconstruct 3D mineralized tissue architecture [39]. The bone mineral density (BMD), bone tissue volume fraction (BV/TV), structure model index (SMI), connective density (Conn. D.), trabecular number (Tb. N), trabecular thickness (Tb. Th), and trabecular separation (Tb. Sp) were quantified [40].

2.3.4. Serum markers measurement

Serum were collected before euthanasia and stored at -80˚C. Bone formation marker amino-terminal propeptide of type I collagen (PINP) and bone resorption marker carboxy-terminal telopeptide (CTX) were assayed using enzyme-linked immunosorbent assay (ELISA) kits (IDS Ltd., Boldon, UK). Serum Mg was assayed using Mg LiquiColor® kit (Stanbio Laboratory, Texas, USA) and serum vitamin C was assayed using Ascorbic Acid Assay Kit II (MAK075, Sigma-Aldrich) according to the company instructions. Serum TNFα were quantified using TNF alpha Rat ELISA Kit (BMS622, Invitrogen).

2.3.5. Histological and histomorphometry analysis

The proximal and distal femora, proximal and distal tibiae were decalcified by 10% EDTA (pH7.4), embedded in paraffin and cut into 5-μm-thick sections along the coronal plane using our established protocol [25,41]. Sections were stained with H&E. Tartrate-resistant acid phosphatase (TRAP) staining (Sigma Diagnostics, Missouri, USA) was performed for counting osteoclast. Proximal femora samples (at week 2) were stained with terminal deoxynucleotidyl transferase dUTP nick end labeling (TUNEL) for apoptosis detection (#11684795910 Roche Applied Science, Rotkreus, Switzerland). The DNA oxidative damage marker 8-Hydroxy-2′-deoxyguanosine (8-oxo-dG) in bone marrow was tested by immunohistochemistry (IHC) with Anti-8-Hydroxy-2′-deoxyguanosine antibody [N45.1] (ab48508, abcam). CD31 was stained as vascular marker in sinusoids and capillaries in bone marrow with anti-CD31 antibody [TLD-3A12] (ab64543, abcam). TNFα was stained as local inflammation marker in bone marrow with *anti*-TNF alpha antibody (ab6671, abcam). To verify the CS effect on IGF-1 expression *in vivo*, IGF-1 was staining in bone marrow with *anti*-IGF-1 antibody (ab40657, abcam). The IHC staining was quantified by staining intensity/stained area using ImageJ (version 1.51, Wayne Rasband, National Institute of Heath, USA).

Histological images were digitalized with a microscopic imaging system (Leica DM5500; Leica Micro-systems, Wetzlar, Germany). The presence of ON was examined with the established criteria, i.e. diffused presence of empty lacunae or pyknotic nuclei of osteocytes in trabecular bone accompanied by surrounding necrotic bone marrow [25]. The rat with at least one ON lesion in proximal femur, distal femur, proximal tibia or distal tibia was considered as ON+ rat, while that with no ON lesion was considered as ON- rat. Histomorphometric analysis was carried out on the metaphysis of proximal tibia in a 2 mm width area 2 mm below the growth plate using OsteoMeasure Histomorphometry System (Osteometrics, Atlanta, GA, USA) according to a standard histomorphometry protocol [42].

2.3.6. Ex vivo cell culture experiments

2.3.6.1. Primary bone mesenchymal stem cells (BMSCs) isolation and osteoblastic differentiation. Given trabecular osteoblasts were differentiated from BMSCs, we cultured BMSCs of rats from every group to compare the osteoblastic differentiation potentials among groups (n = 4 rats/group). Briefly, just after the euthanasia, bone marrow from bilateral femora of each rat was obtained and cultured in α-MEM (12571, Gibco™, Thermo Fisher Scientific) with 10% fetal bovine serum (FBS), 1% Penicillin-Streptomycin-Neomycin (PSN) Antibiotic Mixture (15640055, Gibco™, Thermo Fisher Scientific), at 37 ˚C containing 5% CO_2 for 3 days. Cells were washed and passaged into 6-well plates (100000 cells/well) for 2 days and then differentiated in osteogenic induction medium with 10 nM Dexamethasone, 50 mg/L VC, and 5 mM β-Glycerophosphate.

2.3.6.2. Primary bone marrow-derived macrophages (BMMs) isolation and osteoclastic differentiation. BMMs of rats from each group were cultured (n = 4 rats/group). Briefly, just after the euthanasia, bone marrow from bilateral femora of each rat was obtained and cultured in α-MEM (12571, Gibco™, Thermo Fisher Scientific) with 10% FBS, 1% PSN Antibiotic Mixture (15640055, Gibco™, Thermo Fisher Scientific) at 37 ˚C containing 5% CO_2 for 4 h. Un-adherent cells were transferred and cultured in α-MEM with 20 ng/ml macrophage colony-stimulating factor (M-CSF) for 48 h. Then Cells were passaged to 24-well-plate (200000/well) with 20 ng/ml M-CSF and 20 ng/ml RANKL for 72 h for osteoclastic differentiation. For quantification of osteoclasts, TRAP positive large multinucleated cells (at least three nuclei) were counted (8 microscope images were counted for each cell well and 3 wells were cultured for each animal).

2.4. Quantitative real-time PCR (qRT-PCR) analysis

Total RNA was isolated with RNeasy Mini Kit (Qiagen, USA). Then cDNA was got from reverse transcription using the PrimeScript RT Reagent Kit with gDNA Eraser (TaKaRa). The primer sequences (Tech Dragon Ltd.) are listed in Table S1. qRT-PCR was performed using SYBR® Premix Ex Taq™ (Tli RNaseH Plus, TaKaRa) and further processed using a QuantStudio™ 12 K Flex Real-Time PCR system (Life Technologies, Thermo Fisher Scientific). Relative expression was calculated using the $2^{-\Delta\Delta CT}$ method by normalizing with house-keeping gene GAPDH.

2.5. Statistical analysis

The incidence of ON in every group was defined as the number of ON+ animals divided by the total animal number and analyzed with Chi-square test. All numeric data were expressed as mean ± SD with one-way ANOVA (for comparison of normal control and other SAON treatment groups), or two-way ANOVA (for analysis of Mg/VC treatment), or three-way ANOVA (for comparison of Mg/VC treatment at different time-points) followed by *post-hoc* Bonferroni's multiple comparisons tests to assess statistical significance. Correlation of clinical serum Mg level and duration of CS therapy was analyzed by Pearson's correlation. Statistical analysis was performed using SPSS 17.0 software (Chicago, IL, USA). $p < 0.05$ was considered significant.

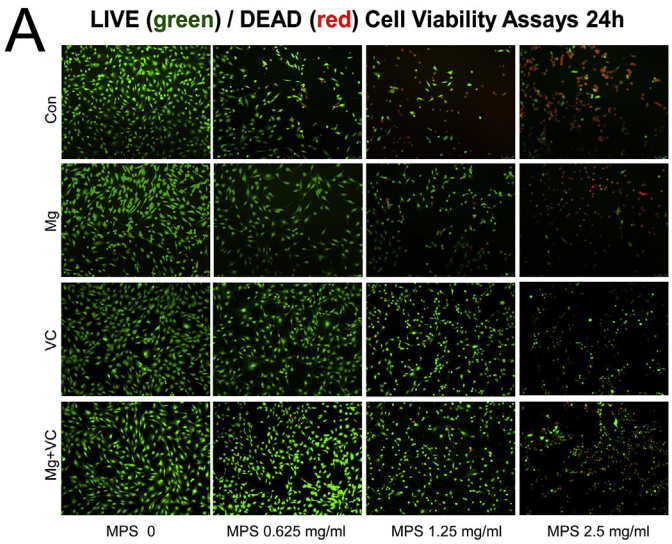

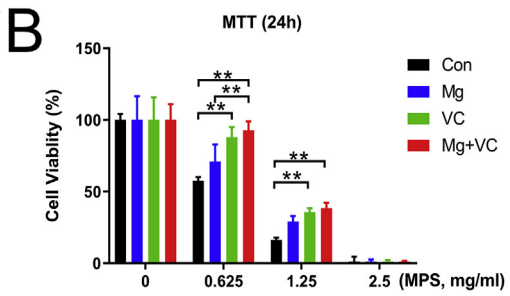

Three-way ANOVA

Source of Variation	P value	P value summary
MPS	<0.0001	****
Mg	0.0026	**
VC	<0.0001	****
MPS x Mg	0.0257	*
MPS x VC	<0.0001	****
Mg x VC	0.0923	ns
MPS x Mg x VC	0.4093	ns

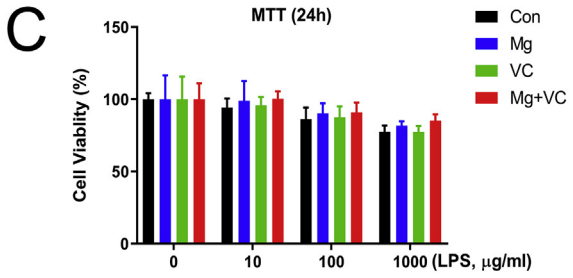

Three-way ANOVA

Source of Variation	P value	P value summary
LPS	<0.0001	****
Mg	0.0230	*
VC	0.5031	ns
LPS x Mg	0.5687	ns
LPS x VC	0.9811	ns
Mg x VC	0.8279	ns
LPS x Mg x VC	0.9622	ns

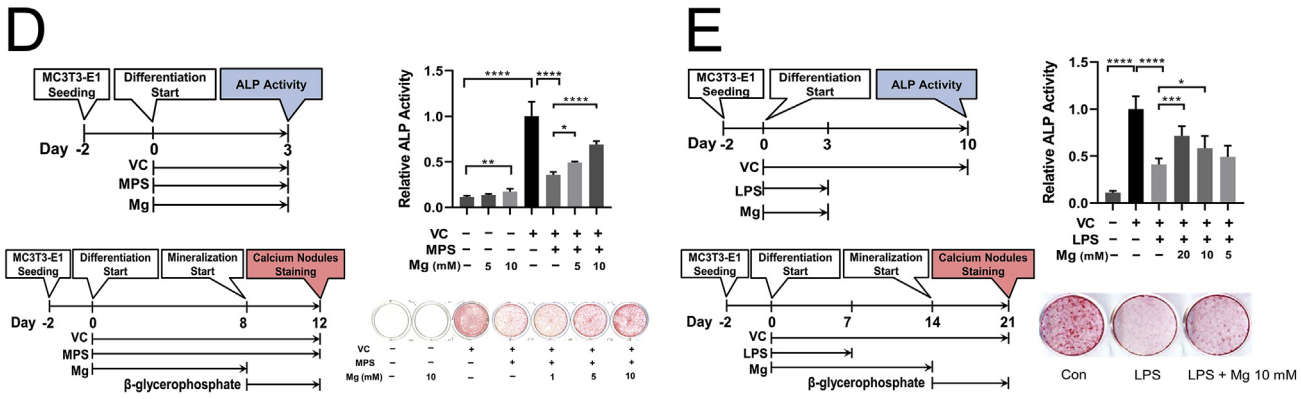

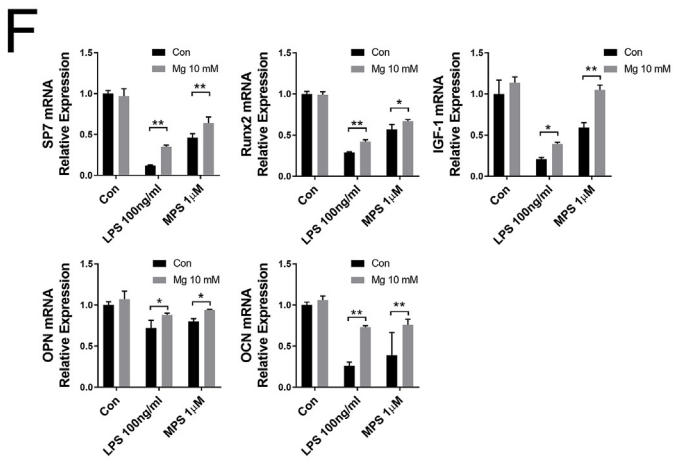

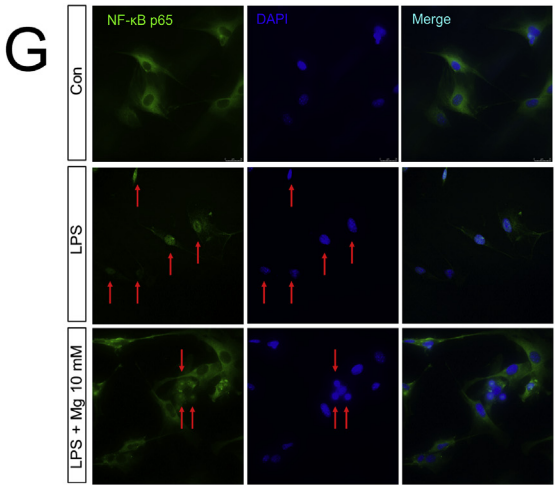

Fig. 1. Effect of Mg and VC on osteoblast cell line MC3T3-E1. (A) Representative live/dead cell staining images. (B) and (C) MTT cell viability assays. (**$p < 0.01$, n = 8). (D) ALP activity and calcium nodules staining showed the effect of Mg and VC on osteoblast differentiation affected by MPS. (E) VC and Mg effect on ALP activity and calcium deposition affected by LPS. (F) qPCR results about SP7, Runx2, OPN, OCN and IGF-1 mRNA expression 24 h after LPS/MPS treatment. (G) IF staining showed anti-inflammation effect of Mg on LPS treated MC3T3-E1. (*$p < 0.05$, **$p < 0.01$, ****$p < 0.0001$, n = 4).

3. Results

3.1. Mg and VC protect MC3T3-E1 osteoblast cell viability affected by MPS/LPS

Live/Dead cell staining and MTT assay correspondingly showed that high dose of MPS (0.625, 1.25 and 2.5 mg/ml, i.e., 1.25, 2.5, 5 mM) inhibited MC3T3-E1 osteoblast cell viability in a dose-dependent manner. Mg and VC supplementation could protect osteoblast cell viability affected by MPS *in vitro* (Fig. 1A and B). MTT assay and three-way ANOVA showed that LPS could decrease MC3T3-E1 osteoblast cell viability, while unlike MPS, even high dose of LPS (1000 μg/ml) could not induce cell death after 24 h treatment. Mg could protect osteoblast cell viability affected by LPS *in vitro* (Fig. 1C).

3.2. VC is essential for Mg to promote osteoblast differentiation affected by MPS/LPS

Calcium Nodules staining showed that the MC3T3-E1 osteoblast cell line could not differentiate to have calcium deposition function without VC supplementation. Mg alone at 10 mM concentration could increase ALP activity 3 days after treatment with statistically significance ($p < 0.01$), while the relative ALP activity was still at low level, i.e., 17% of positive control when compared to that with VC treatment. However, without VC treatment, Mg could not induce calcium deposition. VC supplementation significantly increased the ALP activity. In the VC supplementation condition, 1 μM MPS inhibited ALP activity and calcium deposition, and Mg promoted ALP activity and calcium deposition affected by MPS in a dose dependent manner (Fig. 1D). In the VC supplementation condition, 100 ng/ml LPS significantly inhibited ALP activity and calcium deposition, and Mg promoted ALP activity and calcium deposition affected by LPS (Fig. 1E). Realtime qPCR results showed that 24 h after LPS/MPS treatment, the osteoblast differentiation marker genes SP7, Runx2, OPN and OCN were significantly inhibited, and IGF-1 mRNA expression was significantly inhibited, while Mg supplementation promoted the expression of those genes (Fig. 1F). IF staining showed that nuclear translocation of NF-κB p65 was observed in MC3T3-E1 cells 24 h after LPS stimulation, and Mg treatment decrease the portion of nuclear translocation of active NF-κB p65 (Fig. 1G).

3.3. Mg inhibits osteoclast differentiation in the RAW264.7 cell line and regulates Ca signal

TRAP staining showed that with RANKL treatment, the RAW264.7 cell line differentiated to TRAP-positive multinucleated osteoclasts. VC treatment significantly promoted the number of formed osteoclasts and the mRNA expression of osteoclast marker gene Cathepsin K. Mg treatment significantly reduced the number of RANKL-induced osteoclasts and the Cathepsin K mRNA expression (Fig. 2A).

To further verify the Mg inhibiting effect on osteoclast differentiation and function, two kinds of osteoclastogenesis inducers LPS and RANKL were used. Mg could significantly reduce the number of LPS-induced osteoclasts and RANKL-induced osteoclasts and the NFATc1 (nuclear factor of activated T cells c1) and Cathepsin K mRNA expression after 4 days' treatment (Fig. 2B). Mg could significantly reduce the functional resorption pit area induced by both LPS and RANKL after 6 days treatment (Fig. 2C). IF staining and WB consistently showed that the NF-κB p65 nuclear translocation was decreased by Mg treatment at both LPS and RANKL induced conditions after 30 min treatment (Fig. 2D). To exam if Mg could regulate changes in LPS and RANKL induce Ca^{2+} response, we performed live cell Ca^{2+} imaging on cultured RAW264.7 cell line. Both LPS and RANKL could instantly increase intracellular Ca^{2+} concentration. When added Mg, the increased intracellular Ca^{2+} concentration induced by LPS/RANKL was decreased instantly. There was no intracellular Ca^{2+} response induced by LPS/RANKL when the cells were incubated in Ca^{2+} free medium. NMDG-Cl pretreatment had no effect on LPS/RANKL induced intracellular Ca^{2+} response, while $MgCl_2$ pretreatment could significantly inhibit LPS/RANKL induced intracellular Ca^{2+} response (Fig. 3A and B).

3.4. Serum Mg of ON patients

In our clinical Mg investigation, the two hypomagnesaemia cases with serum Mg levels < 0.76 mmol/L were both from the group of SAON patients being treated with CS (taken up 28.6% (2/7) cases), while the serum Mg levels of patients in other groups were all above 0.80 mmol/L. Statistical analysis showed significantly lower serum Mg in SAON patients being treated with CS when compared to those with CS used before and other ON patients, and there was a significant negative correlation found between serum Mg and the duration of CS therapy. (Fig. S1).

3.5. Mg/VC supplementation increases serum Mg/VC

Serum Mg of SAON group was significantly lower at week 2 and 6 than normal, while Mg supplementation significantly increased the serum Mg level to normal level. Serum VC in SAON group was significantly lower than normal at week 2, while VC supplementation significantly increased the serum VC level at both week 2 and 6 when compared to SAON group (Fig. S2).

3.6. Effect of Mg and VC on SAON in vivo

SAON was identified by histological evaluation. All the SAON model rats developed ON at 2 weeks after induction, indicated by the empty lacunae in trabecular bone or pyknotic nucleus of osteocytes with 100% incidence of SAON (8/8). Mg, VC or their combination could not fully prevent the incidence of SAON at 2 weeks after induction (7/8 for Mg, 7/8 for VC, and 6/8 for combination). The incidence of SAON decreased at 6 weeks after induction. VC and combination could significantly decrease the incidence SAON 6 weeks after induction (Fig. 4A and B).

3.7. Mg and VC suppress the apoptosis of osteocytes

Quantitative analysis of TUNEL staining images showed that the rate of apoptosis of osteocytes at femoral head in SAON model group 2 weeks after SAON induction was significantly higher than that of normal control group (SAON: 52.9% vs. Normal: 3.8%). The apoptotic rate of osteocytes was significantly reduced to 31.4% in Mg group, 37.8% in VC group, and 17.8% in combination group. Two-way ANOVA showed that both Mg and VC could significantly decrease the rate of apoptosis of osteocytes 2 weeks after SAON induction and there was no interaction between Mg and VC in suppressing the apoptosis of osteocytes (Fig. 4C and D).

3.8. Effect of Mg and VC on bone metabolism in vivo

Histomorphometry on week 2 samples showed significantly higher osteoclast number in SAON group when compare to normal group; lower osteoclast number in Mg/VC/combine group when compare to SAON group, and the lowest was in combine treatment group. The osteoblast surface (Ob. S/BS) in SAON group was significantly lower when compare to normal group; and both Mg and VC could significantly increase the osteoblast surface. There was significantly higher marrow fat area fraction in SAON group, and Mg could significantly decrease bone marrow fat area fraction (Fig. 5A and B). For bone turnover markers, the bone formation marker serum PINP in SAON group were significantly lower at both week 2 and week 6 than those in normal group; VC could significantly increase the serum PINP at both week 2 and week 6. The bone resorption marker serum CTX in combine treatment group was significantly lower at week 2 than that in SAON

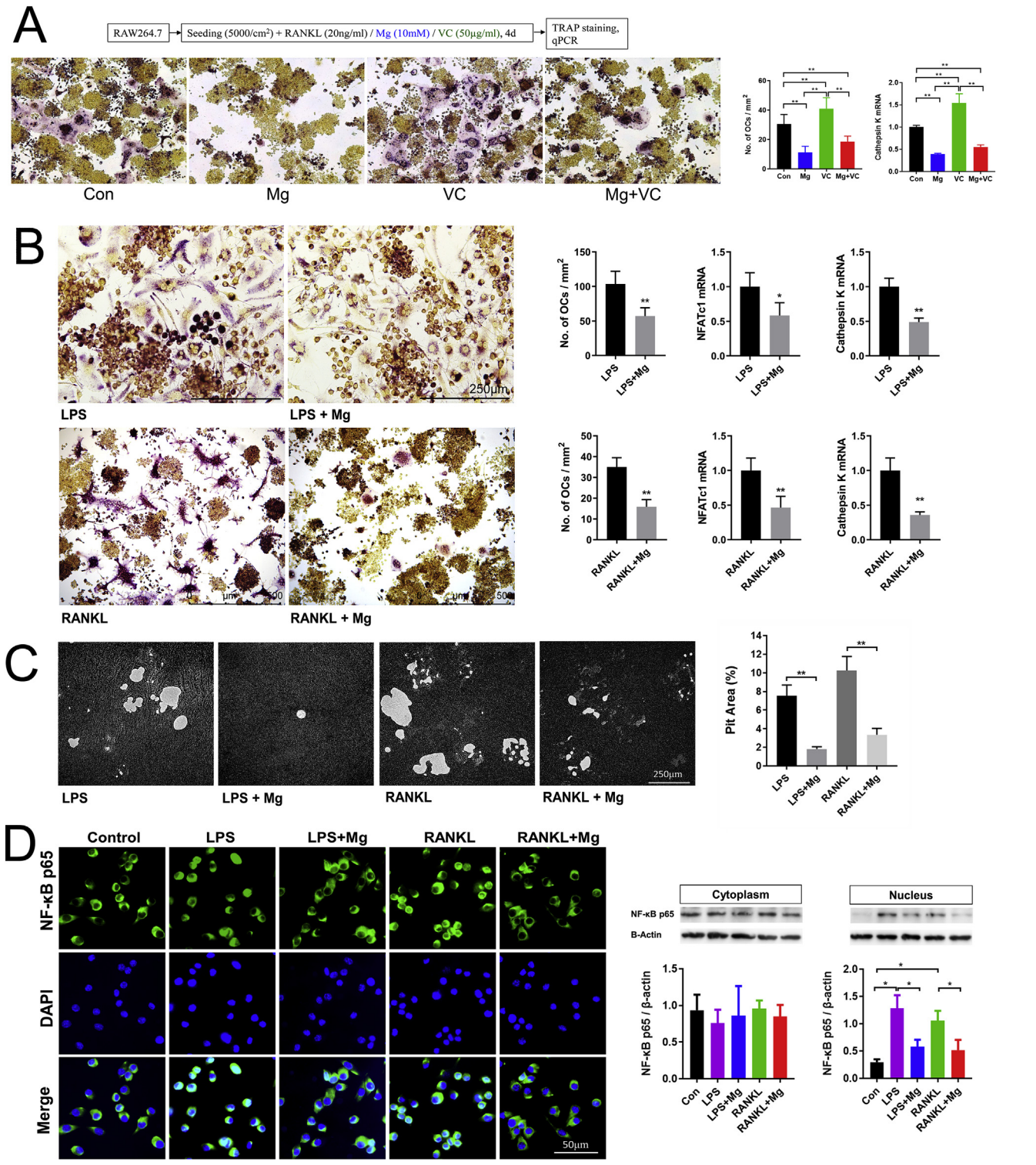

Fig. 2. Effect of Mg and VC on osteoclast cell line. (A) Quantitative of TRAP staining showed differentiated osteoclast number in Mg and VC treated groups, and qPCR showed Cathepsin K mRNA expression in each group. (**$p < 0.01$, n = 4). (B) Quantitative of TRAP staining showed the inhibiting effect of Mg on differentiated osteoclast number at both LPS and RANKL induced conditions, and qPCR showed the inhibiting effect of Mg on NFATc1 and Cathepsin K mRNA expression at both LPS and RANKL induced conditions. (*$p < 0.05$, **$p < 0.01$, n = 4). (C) Pit formation assay showed the inhibiting effect of Mg on the function of osteoclasts at both LPS and RANKL induced conditions. (**$p < 0.01$, n = 4). (D) IF staining and WB showed the inhibiting effect of Mg on NF-κB p65 nuclear translocation at both LPS and RANKL induced conditions. (*$p < 0.05$, n = 4).

group at the same time point (Fig. 5C and D). Trabecular architecture of proximal tibia 6 weeks after SAON induction was analyzed using micro-CT. The bone mineral density (BMD), bone volume fraction (BV/TV), connective density (Conn.D.), and trabecular number (Tb. N) of SAON group were all significantly lower and the trabecular separation (Tb.Sp) of SAON group was significantly higher than that in the normal group. Two-way ANOVA showed that Mg could significantly increase BMD and VC could significantly increase BMD and recover trabecular

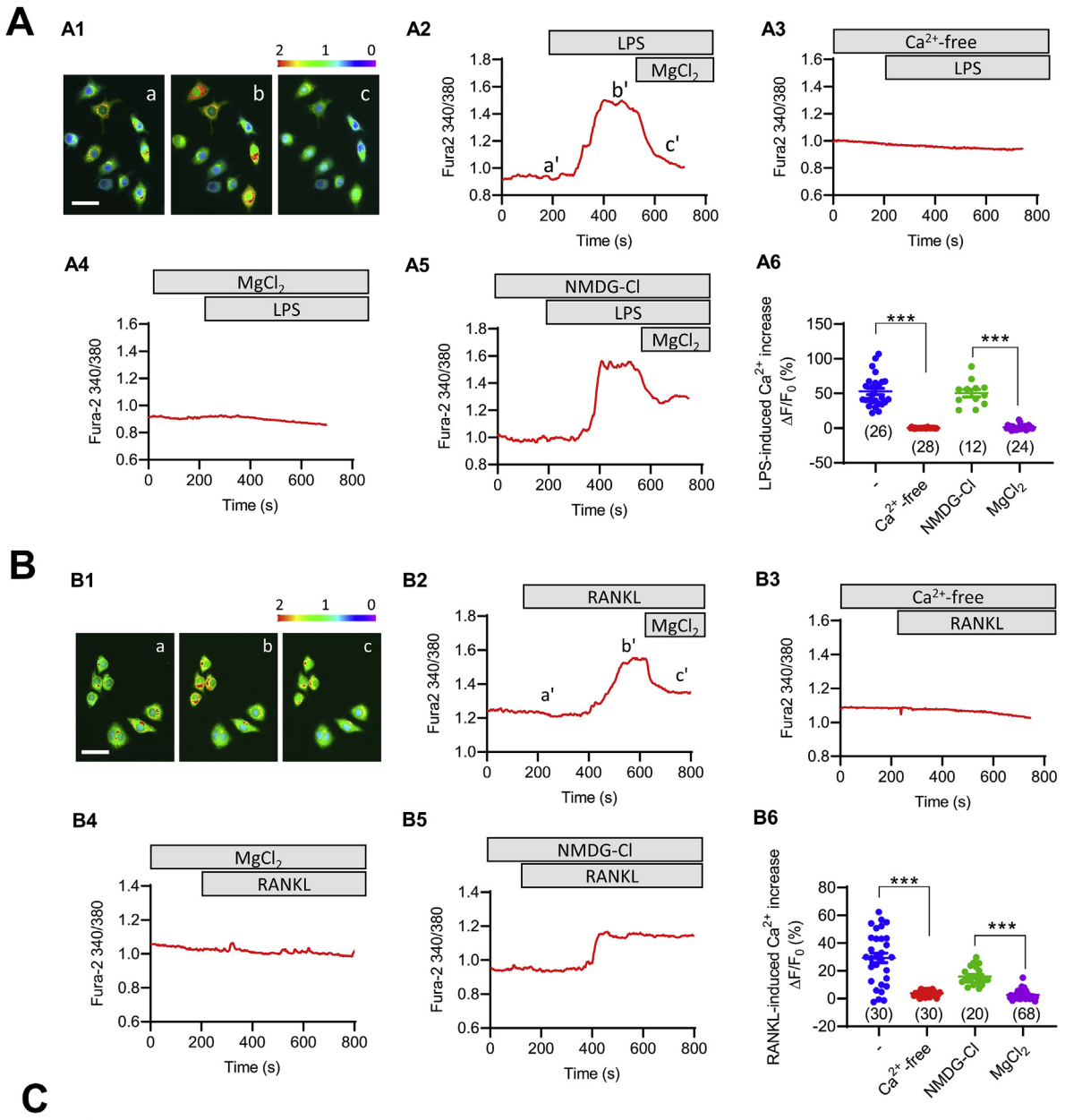

(caption on next page)

Fig. 3. Mg inhibits osteoclast differentiation through regulating Ca signal. (A) Mg blocks LPS-induced intracellular Ca^{2+} increase in RAW264.7 cells. A1-A2) Representative Fura-2 fluorescence images (A1) and corresponding time-course traces (A2) of intracellular Ca^{2+} measurement in RAW264.7 cells before (a) and after adding LPS (100 ng/ml, b) and subsequently $MgCl_2$ (10 mM, c) into a normal bath solution. White bar, 30 μm. Pseudo-colors from purple/blue to red indicate Fura-2340/380 nm ratio from low to high. A3-A5) Representative time-course traces of cells pretreated with Ca^{2+}-free (A3), $MgCl_2$ (10 mM, A4), or NMDG-Cl (20 mM, a non-permeable cation control, A5) before the addition of LPS. A6) Summary of LPS-induced intracellular Ca^{2+} change in RAW264.7 cells under different conditions. (B) Mg blocks RANKL-induced intracellular Ca^{2+} increase in RAW264.7 cells. B1–B2) Representative Fura-2 fluorescence images (B1) and corresponding time-course traces (B2) of intracellular Ca^{2+} measurement in RAW264.7 cells before (a) and after adding RANKL (50 ng/ml, b) and subsequently $MgCl_2$ (10 mM, c) into a normal bath solution. White bar, 30 μm. Pseudo-colors from purple/blue to red indicate Fura-2340/380 nm ratio from low to high. B3–B5) Representative time-course traces of cells pretreated with Ca^{2+}-free (B3), $MgCl_2$ (10 mM, B4), or NMDG-Cl (20 mM, a non-permeable cation control, B5) before the addition of RANKL. B6) Summary of RANKL-induced intracellular Ca^{2+} change in RAW264.7 cells under different conditions. ***$p < 0.001$ by *t*-test; n is shown for each group. (C) Illustration of the pathway of Mg in inhibiting LPS/RANKL induced osteoclast differentiation.

architecture in this SAON model (Fig. 5E).

3.9. VC promotes the potential of osteoblastogenesis of MSCs, and Mg decreases the potential of osteoclastogenesis of BMMs

The bone marrow MSCs of rats from every group at week 2 were cultured *ex vivo*, and then differentiated in osteogenic induction medium. Results showed that the potential of osteogenic differentiation in SAON group was significantly lower than normal. VC could significantly elevate the potential of osteogenic differentiation (Fig. 6A).

The bone marrow macrophages (BMMs) of rats from every group at week 2 were cultured *ex vivo*, and then differentiated in osteoclastic induction medium. Results showed that the osteoclast number in SAON group was significantly higher than normal, while the osteoclast size of SAON group was significantly smaller than normal. VC supplementation could significantly enlarge the osteoclast size and total Cathepsin K mRNA expression, while Mg supplementation could decrease the osteoclast number and total Cathepsin K expression combined with VC when compared with VC group (Fig. 6B).

3.10. Mg promotes angiogenesis and prevents vessel leakages

Vessel architecture in proximal tibia and distal tibia in each group was analyzed by Microfil perfusion and micro-CT scan. Histogram showed that in proximal tibia, the medium-sized (100–200 μm) blood vessels in SAON group were significantly less compared to normal group; Mg could significantly increase the medium-sized blood vessels when compared to SAON group. In distal tibia, the small-sized

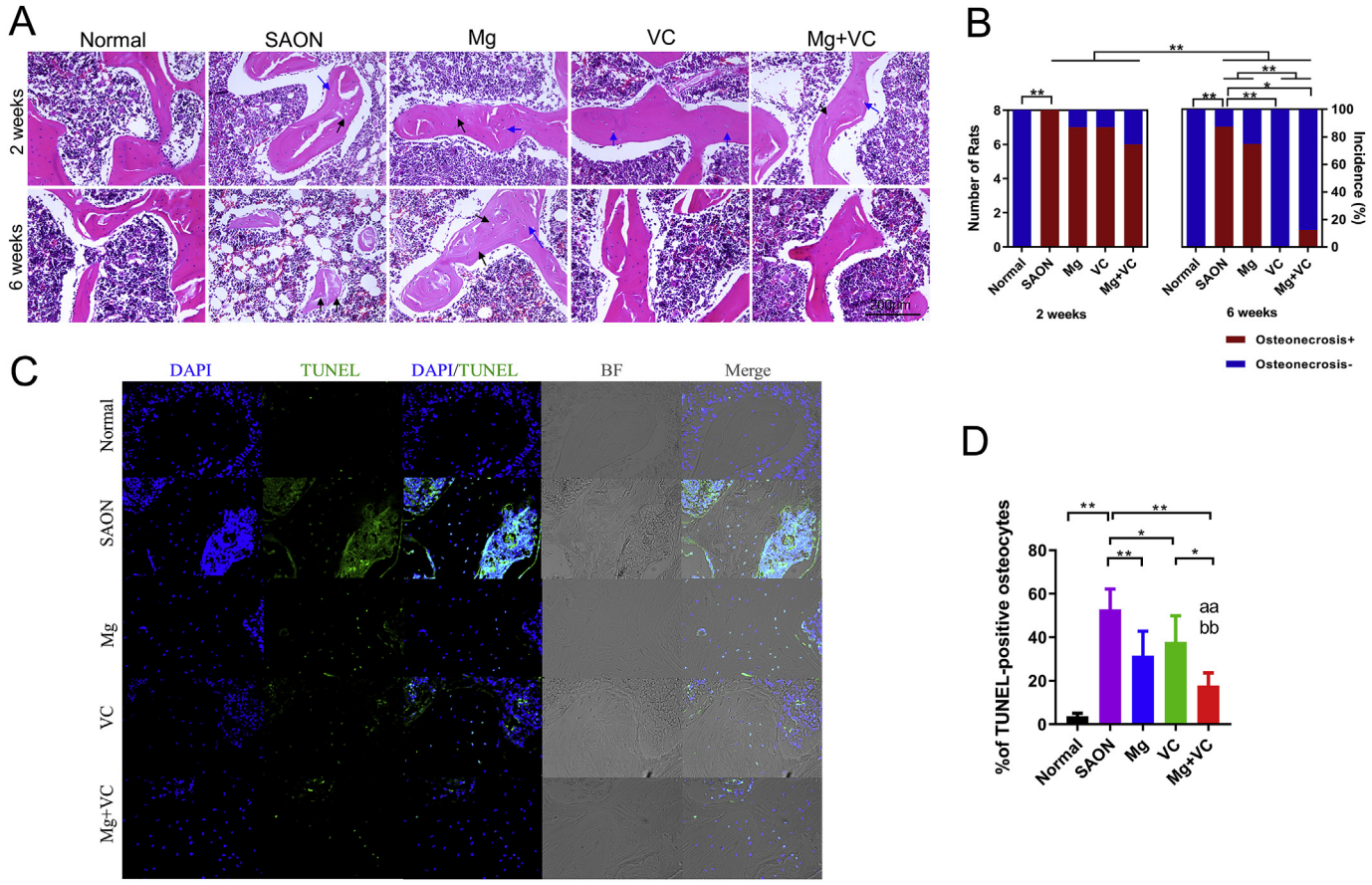

Fig. 4. Effect of Mg and VC on prevention of SAON and suppress the apoptosis of osteocytes. (A) Representative H&E staining images showed ON, indicated by the empty lacunae (black arrow) in trabecular bone or pyknotic nucleus of osteocytes (blue arrow). (B) The incidence of SAON in each group. All the SAON model rats developed ON at 2 weeks after induction. The incidence of SAON decreased at 6 weeks after induction, suggested progressive repair after week 2. VC further significantly decreased the incidence SAON at 6 weeks after induction. (*$p < 0.05$, **$p < 0.01$; Chi-square test, n = 8; osteonecrosis+: with osteonecrosis detected by histology; Osteonecrosis-: without osteonecrosis detected by histology) (C) Representative TUNEL staining images showed apoptosis of osteocytes. (D) Apoptosis rate indicated by percentage of TUNEL-positive osteocytes. (*$p < 0.05$, **$p < 0.01$; one-way ANOVA; aa: $p < 0.01$, for Mg factor; bb: $p < 0.01$, for VC factor, two-way ANOVA; n = 8).

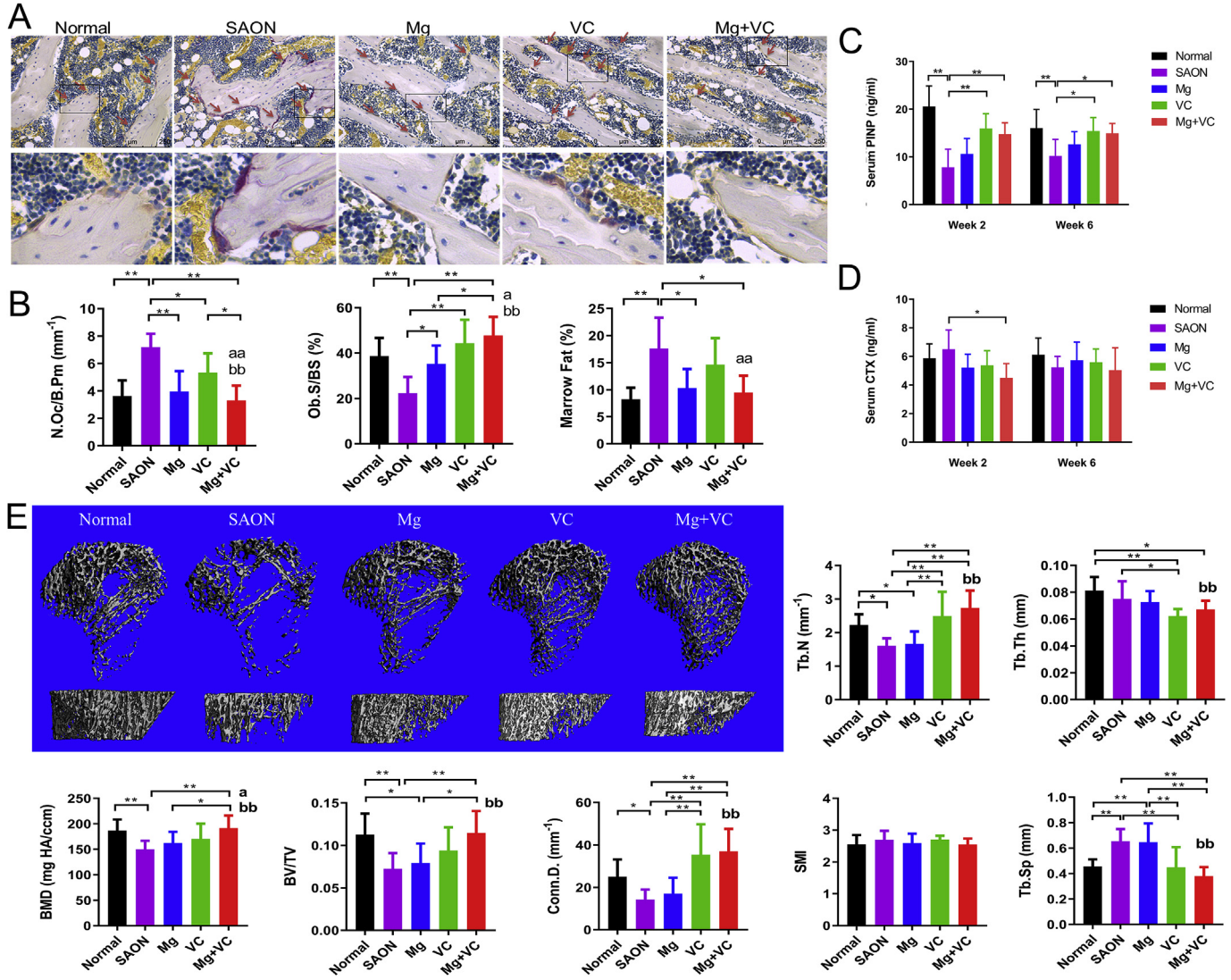

Fig. 5. Effect of Mg and VC on bone metabolism *in vivo*. (A) Representative TRAP staining images showed osteoclasts (red arrow). (B) Histomorphometry results showed osteoclast number (N.Oc/B.Pm), osteoblast surface (Ob. S/BS) and bone marrow fat area fraction in each group. (*$p < 0.05$, **$p < 0.01$; a: $p < 0.05$, aa: $p < 0.01$ for Mg factor; bb: $p < 0.01$ for VC factor; two-way ANOVA; n = 6). (C) bone formation marker PINP and (D) bone resorption marker CTX (*$p < 0.05$, **$p < 0.01$, two-way ANOVA; n = 6). (E) Representative 3D images of micro-CT based trabecular bone of proximal tibia at 6 weeks after SAON induction. (B) Quantitative analysis of the bone mineral density (BMD), bone volume fraction (BV/TV), connective density (Conn. D.), trabecular number (Tb. N), trabecular thickness (Tb. Th) and the structure model index (SMI) in each group. (*$p < 0.05$, **$p < 0.01$; a: $p < 0.05$ for Mg factor; bb: $p < 0.01$ for VC, two-way ANOVA; n = 8).

(< 100 μm) leakage particle proportion of SAON group was significantly larger than that of normal group; and Mg could significantly decrease the proportion of small-sized leakage particles (Fig. 7A). For *in vitro* angiogenesis, scratch-wound healing assay showed that Mg could promote endothelial cell migration in a dose-dependent manner, and the 10 mM concentration of Mg ion had the most promotive effect. Then the 10 mM concentration of Mg ion was tested for the tube formation experiment, and it showed the significant promotion effect (Fig. 7B and C). Transwell permeability assay showed that when treated with LPS, the HUVEC monolayer showed significantly increased leakage for FITC-dextran. Mg supplementation could reduce HUVEC monolayer leakage induced by LPS (Fig. 7D). Co-staining of ZO-1 and NF-κB p65 showed that in the control group, the HUVEC monolayer displayed a cobblestone pattern of the ZO-1 tight junction, and p65 were mainly stayed at cytoplasm. When treated with LPS, some ZO-1 proteins left apart from cell-cell junction and accumulated into nucleus, and the p65 of the same cells were coincidentally activated into nucleus. Mg supplementation protected the ZO-1 cell-cell tight junction and inhibited the p65 activation induced by LPS (Fig. 7E).

3.11. Mg and VC have anti-inflammation, anti-oxidative and anabolic effects in vivo

IHC staining showed significantly higher TNFα locally in bone marrow of SAON group than normal at both week 2 and week 6 after SAON induction, and significantly lower TNFα in Mg/VC/combine group than SAON at both week 2 and week 6 after SAON induction (Fig. 8A). ELISA test showed significantly higher serum TNFα level in SAON group, and Mg could significantly decrease the systemic TNFα level at both week 2 and week 6 after SAON induction (Fig. S3).

IHC staining for the DNA oxidative damage marker 8-Hydroxy-2′-deoxyguanosine (8-oxo-dG) showed that oxidative DNA damage in bone marrow in SAON group was significantly higher than normal at both week 2 and week 6 after SAON induction. Both Mg and VC could decrease the oxidative DNA damage in bone marrow (Fig. 8B).

IHC staining showed that the IGF-1 expression in bone marrow was

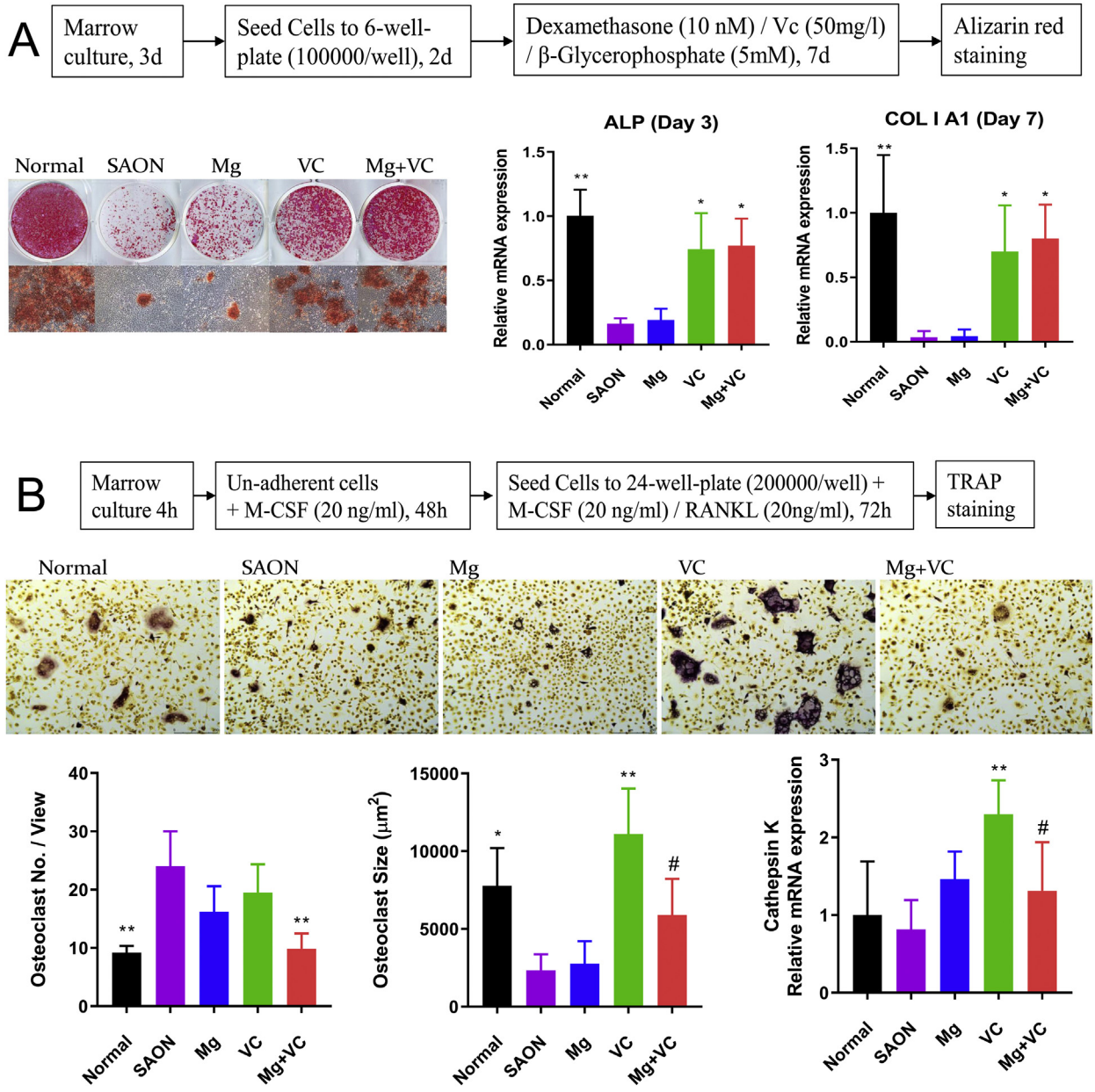

Fig. 6. *Ex vivo* cell culture. (A) The Bone marrow MSCs of rats at 2 weeks after SAON induction from every group were cultured *ex vivo*, and then differentiated in osteogenic induction medium. Representative images of Alizarin red staining and qPCR of ALP and COL I A1 showed the potential of osteogenic differentiation of MSCs in each group. (B) The bone marrow macrophages of rats 2 weeks after SAON induction from every group were cultured *ex vivo* and differentiated in osteoclastic induction medium. Quantitative analysis of TRAP staining images about osteoclast number and size and qPCR of Cathepsin K expression showed the osteoclast differentiation potential of BMMs in each group (*$p < 0.05$, **$p < 0.01$, vs. SAON; #: $p < 0.05$, vs. VC, n = 4).

not obviously changed at week 2 among groups. At week 6 after SAON induction, the IGF-1 expression was significantly lower in bone marrow in SAON group when compared to normal control group, while the IGF-1 expression was significantly higher in Mg/VC/combine group when compared to SAON control group (Fig. 8C).

4. Discussion

The present study demonstrated that supplementation of Magnesium (Mg) and vitamin C (VC) could synergistically alleviate SAON in rats, as supported by the evidence that the incidence of SAON and the ratio of apoptosis of osteocytes in the Mg and VC combination treatment group were both the lowest in all the SAON treated groups at week 2 after SAON induction.

Mg is the fourth abundant element in the body, and the second abundant in the intracellular compartment. It is a co-factor in more than 300 enzymatic reactions involving in energy metabolism and protein and nucleic acid synthesis. Mg also plays an important role in the development of bone and bone metabolism [43]. There is association between low Mg and osteoporosis [44]. There is also association between hypomagnesemia and CS therapy [45], consistent with our clinical data showing lower serum Mg level in SAON patients being treated with CS. The normal adult reference value for serum Mg may vary slightly among different laboratories. A large cross-sectional study in Germany identified hypomagnesaemia if serum Mg levels < 0.76 mmol/L; and subclinical Mg deficiency, based on serum Mg levels < 0.80 mmol/L, is a crisis for many metabolic diseases [46]. Our data suggested that CS treatment could induce Mg deficiency, and the lower serum Mg level was associated with the duration of CS therapy. It is a limitation in our clinical data analysis that all serum data are from ON

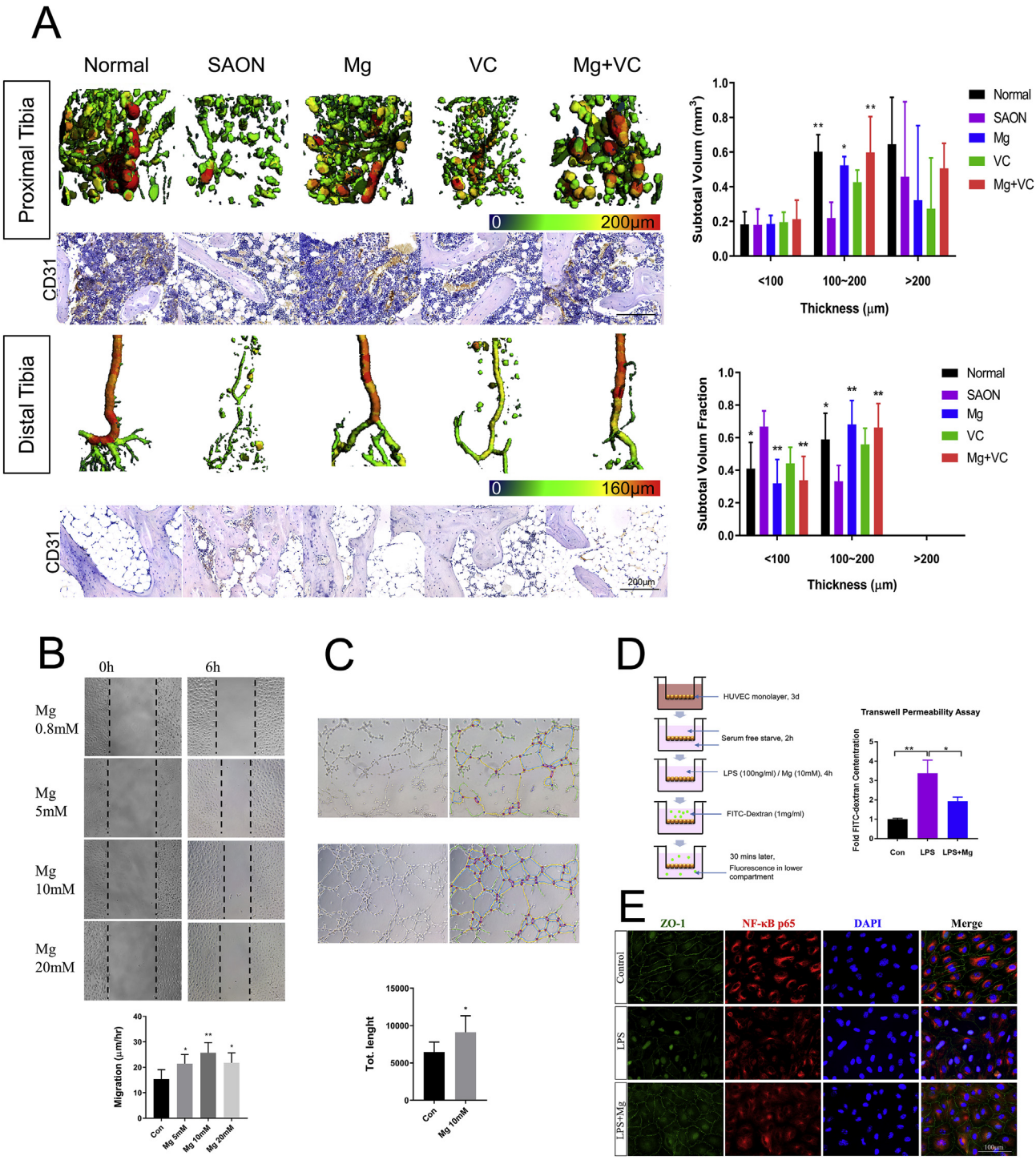

Fig. 7. Mg promotes angiogenesis and reduces vessel leakage. (A) Representative 3D images of micro-CT based vessel architecture and CD31 IHC staining images in proximal tibia and distal tibia 2 weeks after SAON induction in each group. Histogram showed the subtotal volume of the small (< 100 μm), medium (100–200 μm) and large-sized (> 200 μm) blood vessels/perfused microfil in each group in proximal (above) and distal tibia (below) (*p < 0.05, **p < 0.01, n = 4). (B) Effect of Mg on endothelial cell migration. (C) Effect of Mg on endothelial cell tube formation. (*p < 0.05, **p < 0.01, n = 4) (D) Transwell permeability assay showed the effect of Mg on endothelial cell leakage induced by LPS. (E) Co-IF-staining of ZO-1 and NF-κB p65 showed the coincidental effects of Mg on protecting the integrity of endothelial cell monolayer (showed by ZO-1 staining) and reducing the inflammation (showed by NF-κB p65 staining) induced by LPS. (*p < 0.05, **p < 0.01, n = 4).

patients and normal serum Mg level from ON patients without CS treatment was used as reference for the current study instead of using our own normal health control. In the current SAON rat model, results showed significantly lower serum Mg in SAON group at both week 2 and week 6 when compared to normal group, and Mg supplementation elevated the serum Mg level to normal level, which is a novel finding of the current study, suggesting potential clinical significance. There are multifactorial causes of Mg deficiency in patients with CS treatment, including disease determined, low Mg intake, and increased urinary loss of Mg which is a side-effect of CS therapy [16,45].

Hypomagnesemia is associated with CS induced metabolic disorder and SAON development. CS treatment could induce insulin resistance

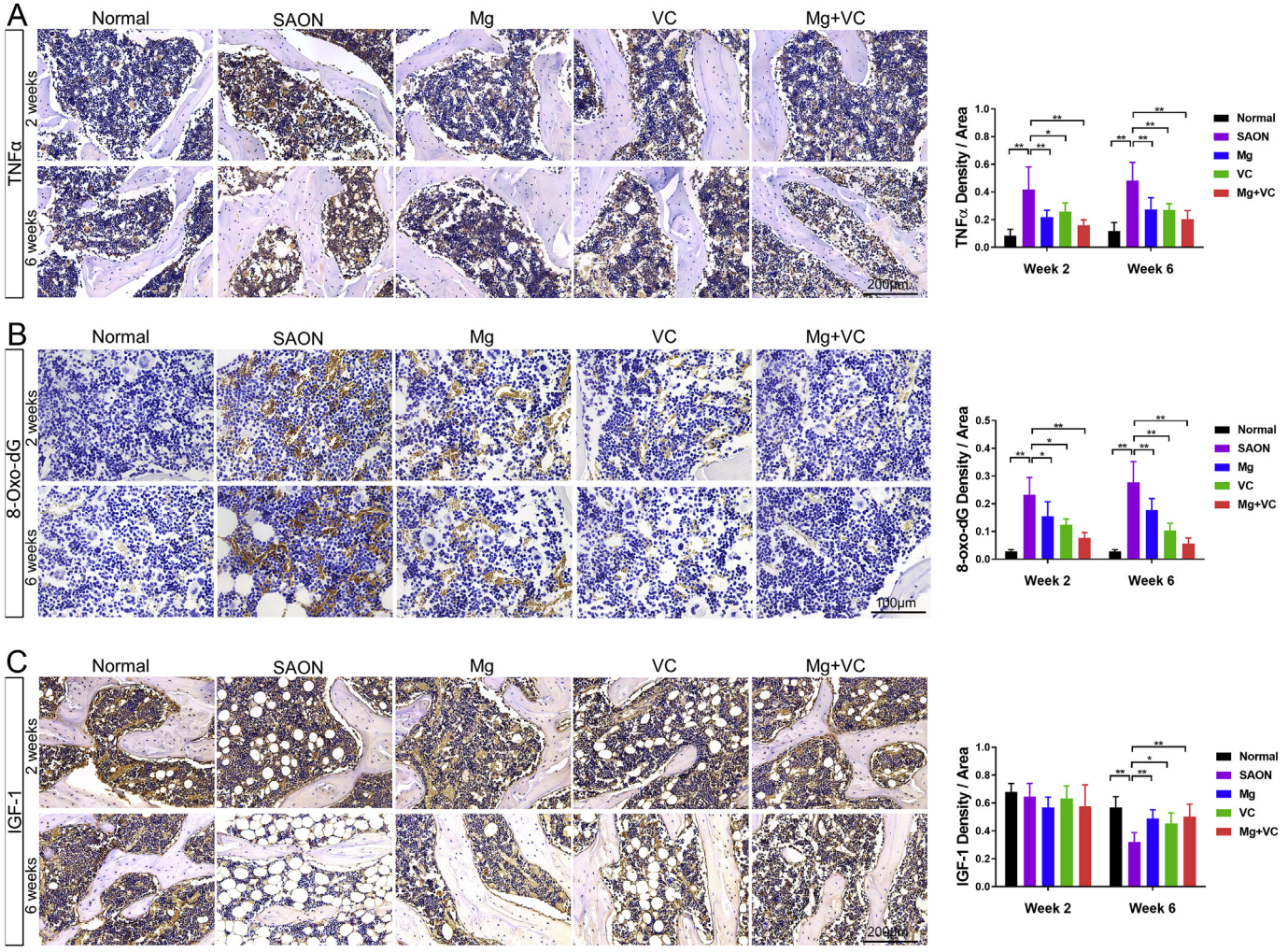

Fig. 8. *In vivo* anti-inflammation, anti-oxidative and anabolic effect and pathways of Mg & VC in preventing SAON. (A) Representative IHC staining images and quantification for TNFα expression in bone marrow. (B) Representative IHC staining images and quantification for 8-Oxo-dG expression in bone marrow. (C) Representative IHC staining images and quantification for IGF-1 expression in bone marrow. (*$p < 0.05$, **$p < 0.01$, n = 6).

by decreasing the activity of osteoblast and decease the secretion of osteocalcin from osteoblast [12,47] as osteocalcin positively regulate insulin sensitivity [48]. Evidence suggested that insulin resistance caused hypomagnesemia mainly due to renal Mg wasting, and Mg deficiency further aggravated insulin resistance [49] as Mg is important for maintaining the affinity of the insulin receptor tyrosine kinase for ATP [50]. Osteocalcin can stimulate angiogenesis [51] while insulin resistance impaired angiogenesis [52] so as the blood flow resulting in hypoxia and consequently SAON. For lipid metabolism, insulin resistance could impair lipoprotein transportation and increase visceral fat and plasminogen activator inhibitor 1 (PAI-1) [53], thus resulting in hypercoagulation and hypofibrinolysis. The increased thrombosis and blood pressure reduce blood flow [54], contributing to the development of SAON as well. Clinically, hypomagnesemia is positively associated with metabolically obese normal weight phenotypes, e.g., hyperglycemia, hypertriglyceridemia, insulin resistance in the non-obese individuals [55], and Mg supplementation improves insulin sensitivity in non-diabetic cases to benefit their body metabolism [56].

Inflammation could stimulate ON. Experimentally, LPS plus CS treatment induced higher SAON incidence than CS treatment only [57]. Clinically, systemic inflammation diseases such as SLE is known with higher incidence of SAON [10]. Of note, LPS treatment alone could also induce ON [58], and inflammatory diseases could develop ON even without CS treatment [59]. It was reported that Mg supplementation had anti-inflammatory effect clinically [60], and experimentally *in vivo* and *in vitro* [61]. Inflammation could decrease osteoblastic bone formation, increase apoptosis of osteoblast and osteocytes, and increase osteoclastic bone resorption [62] to deteriorate the repair progress of SAON. Furthermore, inflammation could increase the permeability of endothelia cells to increase the leakage of blood vessels and edema and pain within the lesions [63]. Our *in vivo* results suggested that Mg supplementation could decrease the apoptosis of osteocytes, increase the osteoblast surface and decrease the osteoclast number, decrease the small-sized blood leakage in yellow bone marrow region, which were associated with its anti-inflammatory effect locally and systemically. Our *in vitro* results indicated that Mg could promote osteoblast differentiation under LPS treatment through anti NF-κB regulated inflammation pathway. It was reported that NF-κB inhibitor could abrogate osteoclast formation [64], consistently our study showed that Mg could inhibit osteoclast differentiation *in vivo* and *in vitro*. Our *in vitro* results suggested that both LPS and RANKL induced osteoclast differentiation through NF-κB signaling pathway, and Mg could inhibit osteoclast differentiation and function through suppressing NF-κB signaling pathway. Our results also suggested that Mg could reduce endothelial cell leakage induced by LPS *in vitro* through suppressing NF-κB signaling pathway. It was reported that Ca ions influx was necessary for NF-κB activation and translocation to nuclear in both macrophages [65] and endothelial cells [66]. Influx of extracellular Ca^{2+} via TRPV4/5 (Transient receptor potential cation channel subfamily V members) channels in cell membrane was also necessary in RANKL induced

osteoclast differentiation [67,68]. Our results showed that both LPS and RANKL could induce Ca^{2+} influx which could be blocked by Mg supplementation, suggesting that Mg could suppressing NF-κB signaling pathway through inhibiting extracellular Ca^{2+} influx, which was the potential underlining mechanisms of the effect of Mg on anti-inflammation and inhibiting osteoclast differentiation induced by the two kinds of inducers LPS and RANKL and then attenuating SAON in the current study (Fig. 3C).

CS has anti-anabolic effects, demonstrating with reduced bone and mineral metabolism, and anti-angiogenesis effect [69]. In contrast, Mg has anabolic effect as Mg ions is involved in ATP synthesis in the mitochondria to regulate energy metabolism and intracellular protein synthesis [70]. Our *in vitro* study showed that Mg could increase IGF-1 expression in osteoblast cell line under MPS treatment. Consistently, our *in vivo* study also showed that Mg/VC could increase IGF-1 expression in bone marrow 6 weeks after SAON induction. Acute injury might induce local IGF-1 expression related from inflammation to reparation [71], so the IGF-1 expression in bone marrow region in SAON group was not found decreased at week 2. IGF-1 expression was reported inversely associated with malnutrition and osteoporosis [72] and bone marrow fat clinically [73], which were consistently with our *in vivo* IHC results at week 6 after SAON induction. IGF-1 is an anabolic hormone inversely related to inflammatory markers (i.e., TNF-α) and oxidative stress [74]. IGF-1 can promote osteoblast cell growth and differentiation through mitochondrial energy metabolism pathways to stimulate bone formation [75]. Also, IGF-1 can stimulate angiogenesis [76]. Clinical evidence showed that the Mg level was strongly and independently associated with total IGF-1 level in the elderly [77]. Previous study showed that Mg supplementation could significantly increase IGF-1 level in Mg-deficient rats [78]. Therefore, the anabolic effect of Mg through increasing IGF-1 signaling pathway could have beneficial effect to antagonize the side-effect of CS treatment and then attenuate the development of SAON.

Compared with the effects of Mg supplementation, VC had more significant effect on promoting osteoblast differentiation, evidenced by osteoblast surface, serum bone formation marker (PINP) and *ex vivo* osteogenic differentiation of BMSCs. In our *in vitro* study, the effect of Mg on osteoblast was controversial, because different cell culture conditions could lead to different results. Our study showed that Mg promoted osteoblast differentiation in the MPS/LPS inhibition condition due to its anabolic effect through promoting IGF-1 pathway and anti-inflammation effect through inhibiting NF-κB pathway. Our results showed that 10 mM Mg in cell culture medium could promote early stage of osteoblast differentiation while inhibit late stage mineralization (Fig. S4). For the mineralization, calcium deposition in the extracellular matrix (ECM) was from intracellular calcium-containing vesicles transported to the ECM [79]. High Mg could inhibit calcium resorption by osteoblast to inhibit mineralization. In order to show the promoting effect, 10 mM Mg was supplemented at early stage of osteoblast differentiation before mineralization in the present study. When β-glycerophosphate was added to induce mineralization at late stage of osteoblast differentiation, no more high concentration of Mg was added in the cell culture medium. Using Mg free DMEM medium (SH30262.01, HYCLONE, USA), we found that when the Mg was supplemented at whole osteoblast differentiation processing, the best mineralization was from 0.8 mM Mg condition (normal concentration), which matched with the *in vivo* study that Mg supplementation could promote osteoblast in MPS/LPS induced lower Mg condition. Osteoblast differentiation includes three stages: BMSC to preosteoblast, osteoblast maturation and mineralization. The *ex vivo* cell culture of BMSCs in same osteogenic cell culture medium reflects the different osteogenic differentiation potentials of BMSCs to preosteoblasts among groups of rats. Our results suggested that VC could promote the potential of osteogenesis of BMSCs, the first stage of osteoblast differentiation, while Mg showed no significant effect at this stage, although Mg showed significant effect in promoting osteogenesis on osteoblast maturation at later stage, evidenced by *in vivo* histomorphometry of osteoblast surface and *in vitro* osteoblast differentiation. The results of quantification of osteoclast number in *ex vivo* cell culture and *in vivo* histomorphometry were consistent in the same trend that VC did not increase osteoclast number. The inconsistence was osteoclast activity showed by TRAP staining of *ex vivo* cell culture and *in vivo* histology. The inconsistence is because of the different osteoclast differentiation conditions between *ex vivo* and *in vivo*. For the *ex vivo* cell culture, the BMMs of rats from each group were cultured in the same osteoclast differentiation medium, the results just showed the potential of osteoclastogenesis of BMMs. While for the *in vivo* condition, early studies reported that the osteoclast differentiation was affected by many factors, e.g., inflammation and oxidative injury could induce osteoclast differentiation [80,81]. Refer to our *in vivo* IHC staining results, VC had anti-inflammation and anti-oxidative effects, suggesting that VC could inhibit the differentiation of osteoclast *in vivo* through its anti-inflammation and anti-oxidative pathways. However, VC had less significant effect on osteoclast number than Mg and had no effect on bone marrow fat area fraction, blood perfusion in red bone marrow region and blood leakage in yellow bone marrow region, while Mg showed significant effects. Our *in vitro* results showed that VC was essential for osteoblast differentiation, which was consistent with previous study [23]. VC deficiency could induce osteoporosis and higher VC intake leaded to higher BMD [23]. Our micro-CT results demonstrated that after VC supplementation for 6 weeks, the BMD and trabecular architecture were significant better than that of the SAON controls, while Mg supplementation could only increase BMD without improving trabecular architecture, suggesting that VC might improve the repair of SAON better than Mg alone at bone quality level. However, Mg ions had more significant effect on regulating metabolism, such as decreasing osteoclast differentiation and bone marrow fat, improving marrow blood perfusion and decreasing vessel leakage found in the present study, which could be explained as the main causes of destructive repair in SAON [82]. SAON is a disordered metabolism disease that involves disorder of different tissues' regulation, such as bone, fat and blood vessel, so combination of Mg and VC exerted the best on attenuate SAON that would suggest the ideal application potential for Mg-based implants to treat SAON in hip-preserving surgery.

The DNA oxidative injury was evaluated by IHC staining of 8-oxo-dG. Our results showed that both Mg and VC supplementation reduced the oxidative stress in bone marrow of SAON induced rats. It was reported that Mg deficiency was associated with oxidative stress in aging and vascular diseases, and the oxidative reactions were contributed by the pro-inflammatory response induced by Mg deficiency [83], so Mg reduces oxidative stress through its anti-inflammation effect indirectly. VC is a physiological antioxidant of outstanding functions for protection against diseases and degenerative processes caused by oxidant stress. VC reduces oxidative stress directly through donating its electrons in the antioxidant reactions to prevent other compounds from being oxidized, and many *in vitro* experiments showed the antioxidant actions of VC [84].

The aim of using biomaterials in early stage of osteonecrosis in hip-preserving surgery is to preserve the function of hip joint without joint-replacement surgery, so it is important to prevent the collapse of femoral head due to activated osteoclastic bone resorption around necrotic lesions. Our study current shows that Mg is more efficient in inhibiting osteoclast differentiation. As we designed, VC works quite well in promoting new bone formation, and there is no necrotic bone at week 6, which also suggests higher bone turnover rate in VC treated groups, while suppression of bone turnover is a therapy strategy to prevent collapse in SAON [85]. The highly mineralized necrotic bone could also maintain mechanical properties in favor of preventing collapse, so the persist presence of necrotic lesions in Mg supplemented groups at week 6 due to the inhibited bone resorption suggests that Mg is not a factor associated with increase of bone turnover. In terms of combined use of Mg (for the inhibiting bone resorption effect) and VC (for the promoting bone formation effect) promote the repair of SAON,

the result could be regarded as the additive effect of Mg and VC. For regulating the disordered metabolism to attenuate SAON, our study suggests that Mg has anti-inflammation effect and VC has anti-oxidative effect underlying the effective SAON prevention. Experimental evidence of others showed that inflammation and oxidative stress could reinforce each other [86,87]. As anti-inflammatory treatment and anti-oxidative treatment have synergistic effects [88], we conclude that there is synergistic interaction between VC (anti-oxidative) and Mg (anti-inflammation).

We use $MgCl_2$ in our *in vitro* study. In the mechanism study NMDG (*N*-methyl-D-glucamine) chloride is used as chloride control to show that Mg ions but not chloride have anti inflammation effect through inhibiting calcium influx. Study of others using both $MgCl_2$ and $MgSO_4$ showed that there was no different effect between the two kinds of Mg ions on osteoblast [89]. Other *in vivo* studies also showed that both $MgCl_2$ [90] and $MgSO_4$ [91] have the same anti-osteoarthritic effect. The special situation for different Mg sources is brain Mg that the Mg supplementation should go through blood-brain barrier to brain. Magnesium-L-threonate (MgT) is a better Mg source to elevate brain Mg [92]. For our current study Mg ions could directly reach bone cells from serum, so we focus on the Mg ions' effect and mechanism although it would be more precise to compare two different Mg ions.

In summary, CS has anti-anabolic effect to negative regulate bone formation and angiogenesis. LPS induced inflammation (mimic inflammatory diseases) decreases bone formation and increases apoptosis and bone resorption; and increases vessel permeability and leakage. Both bone event (bone matrix degeneration) and vessel event (ischemia) induce SAON. CS also induces oxidative stress, which will promote cell death to induce SAON. There is a mutual activation loop among anti-anabolic, inflammation and oxidative stress [74]. CS treatment could induce lower Mg. Mg supplementation increases the serum Mg level to normal level. Mg has anti-inflammatory effect and anabolic effect (e.g. through IGF-1 pathway). VC is an antioxidant and could induce osteogenesis. The combination of Mg and VC exerts synergistic effect for attenuating SAON (Scheme 1).

Nowadays, more and more biodegradable Mg materials are used to treat SAON clinically and preclinically [5,93]. Clinical trial using Mg screw to treat patients with osteonecrosis at femoral head (ONFH) showed that Mg screw improved the fixation of vascularized bone graft at femoral head in ONFH patients. The healing quality was not only assessed by Harris Hip Score (HHS), but also quantitatively evaluated by the displacement of the bone flap. Besides, BMD was found higher around Mg screw and at the fusion region of bone graft with local bone compared to control [5]. Our study supported that besides the mechanical fixation, Mg ions release from Mg crew had its bioactive function for improving of the repair of osteonecrotic lesions. The Mg ion releasing from the biodegradable materials can facilitate the benefit effect to attenuate the side-effect of CS in SAON patients. It is highly encouraged to develop biomaterials releasing Mg and VC that can annulate SAON and promote the repair of SAON in future study. Femoral neck fracture is one of the causes of trauma induced femoral head necrosis due to fracture nonunion [94]. Since Mg could improve bone fracture healing [95], Mg-based internal fixation implant with its degradation and Mg ions release for femoral neck fracture repair has great potential to increase the cortical bone formation in fracture repair enhancement as well as to prevent avascular necrosis suggested by the findings demonstrated by the current experimental study.

In conclusion, the present study demonstrated that Mg and VC supplementation could synergistically attenuate the side-effect of CS treatment and SAON and promote the repair of SAON in a rat model. Our preclinical study lays down a scientific foundation for facilitating combinable supplementation of Mg and VC using biomaterials releasing Mg and VC as potential application for SAON patients. The current research findings may also share the lights on the potential underlying mechanism associated with beneficial effects in skeletal regeneration of using biodegradable Mg-based implants for orthopaedic applications.

Data availability

Supplementary data related to this article were included.

Author contributions

L Qin, L Zheng, L Wang and J Xu conceived and designed the study and wrote the original draft. D Zhao and B Liu collected and interpreted the clinical data. L Zheng, J Wang, J Xu, X Zhang, L Huang, R Zhang, H Zu, X He, J Mi and Q Pang performed experiments and analyzed data. X Wang and Y Ruan assisted with experimental design and data interpretation. L Qin accepted responsibility for the integrity of the data analysis. All revised and edited the manuscript.

Declaration of competing interest

All authors declare that they have no conflict of interest.

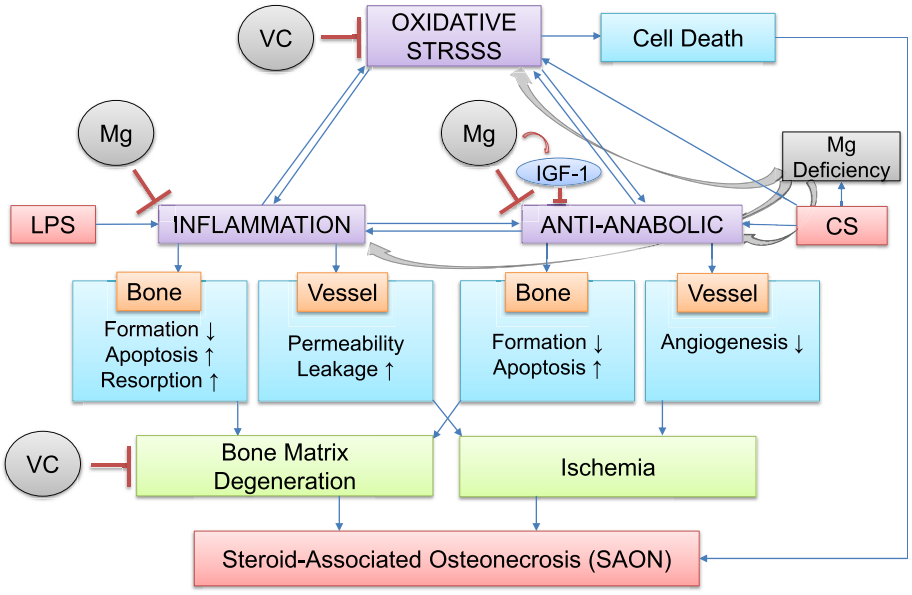

Scheme 1. Illustration of the pathway of Mg and VC in attenuating SAON. CS has its anti-anabolic effect: to negative regulate bone formation and increase apoptosis in bone; and negative regulate angiogenesis. LPS induced inflammation, mimic inflammatory diseases, decreases bone formation and increases apoptosis and bone resorption in bone event; and increases vessel permeability and leakage. Both bone matrix degeneration and ischemia induce SAON. CS also induces oxidative stress, which promotes cell death. There is a mutual activation loop among anti-anabolic, inflammation and oxidative stress. CS treatment could induce Mg deficiency. Mg deficiency is associated with inflammation, oxidative stress, and anabolic defect. Mg supplementation can maintain the serum Mg level at physiological range. Mg has anti-inflammatory effect and anabolic effect (e.g. through IGF-1 pathway). VC is an antioxidant and can induce osteogenesis. The combination of Mg and VC exerts synergistic effect for attenuating SAON.

Acknowledgement

The study was supported in part by Theme-based Research Scheme of Research Grants Council of the Hong Kong Special Administrative Region, PR China (Ref No. T13-402/17-N).

Appendix A. Supplementary data

Supplementary data to this article can be found online at https://doi.org/10.1016/j.biomaterials.2020.119828.

References

[1] D. Zhao, F. Witte, F. Lu, J. Wang, J. Li, L. Qin, Current status on clinical applications of magnesium-based orthopaedic implants: a review from clinical translational perspective, Biomaterials 112 (2017) 287–302.
[2] L. Tian, Y. Sheng, L. Huang, D.H.-K. Chow, W.H. Chau, N. Tang, T. Ngai, C. Wu, J. Lu, L. Qin, An innovative Mg/Ti hybrid fixation system developed for fracture fixation and healing enhancement at load-bearing skeletal site, Biomaterials 180 (2018) 173–183.
[3] L. Tian, N. Tang, T. Ngai, C. Wu, Y. Ruan, L. Huang, L. Qin, Hybrid fracture fixation systems developed for orthopaedic applications: a general review, J. Orthopaed. Transl. 16 (2019) 1–13.
[4] H.-S. Han, S. Loffredo, I. Jun, J. Edwards, Y.-C. Kim, H.-K. Seok, F. Witte, D. Mantovani, S. Glyn-Jones, Current status and outlook on the clinical translation of biodegradable metals, Mater. Today 23 (2019) 57–71.
[5] D. Zhao, S. Huang, F. Lu, B. Wang, L. Yang, L. Qin, K. Yang, Y. Li, W. Li, W. Wang, Vascularized bone grafting fixed by biodegradable magnesium screw for treating osteonecrosis of the femoral head, Biomaterials 81 (2016) 84–92.
[6] C.C. Mok, C.S. Lau, R.W. Wong, Risk factors for avascular bone necrosis in systemic lupus erythematosus, Br. J. Rheumatol. 37 (8) (1998) 895–900.
[7] L.K. So, A.C. Lau, L.Y. Yam, T.M. Cheung, E. Poon, R.W. Yung, K.Y. Yuen, Development of a standard treatment protocol for severe acute respiratory syndrome, Lancet 361 (9369) (2003) 1615–1617.
[8] Z.-R. Li, L.-M. Cheng, K.-Z. Wang, N.-P. Yang, S.-H. Yang, W. He, Y.-S. Wang, Z.-M. Wang, P. Yang, X.-Z. Liu, Herbal Fufang Xian Ling Gu Bao prevents corticosteroid-induced osteonecrosis of the femoral head—a first multicentre, randomised, double-blind, placebo-controlled clinical trial, J. Orthopaed. Transl. 12 (2018) 36–44.
[9] Z.R. Li, W. Sun, H. Qu, Y.X. Zhou, B.X. Dou, Z.C. Shi, N.F. Zhang, X.G. Cheng, D.L. Wang, W.S. Guo, [Clinical research of correlation between osteonecrosis and steroid], Zhonghua wai ke za zhi [Chinese journal of surgery] 43 (16) (2005) 1048–1053.
[10] K. Oinuma, Y. Harada, Y. Nawata, K. Takabayashi, I. Abe, K. Kamikawa, H. Moriya, Osteonecrosis in patients with systemic lupus erythematosus develops very early after starting high dose corticosteroid treatment, Ann. Rheum. Dis. 60 (12) (2001) 1145–1148.
[11] L. Chen, G. Hong, B. Fang, G. Zhou, X. Han, T. Guan, W. He, Predicting the collapse of the femoral head due to osteonecrosis: from basic methods to application prospects, J. Orthopaed. Transl. 11 (2017) 62–72.
[12] C.A. O'brien, D. Jia, L.I. Plotkin, T. Bellido, C.C. Powers, S.A. Stewart, S.C. Manolagas, R.S. Weinstein, Glucocorticoids act directly on osteoblasts and osteocytes to induce their apoptosis and reduce bone formation and strength, Endocrinology 145 (4) (2004) 1835–1841.
[13] R.S. Weinstein, R.L. Jilka, A.M. Parfitt, S.C. Manolagas, Inhibition of osteoblastogenesis and promotion of apoptosis of osteoblasts and osteocytes by glucocorticoids. Potential mechanisms of their deleterious effects on bone, J. Clin. Invest. 102 (2) (1998) 274–282.
[14] G.-J. Wang, D. Sweet, S.I. Reger, R.C. Thompson, Fat-cell changes as a mechanism of avascular necrosis of the femoral head in cortisone-treated rabbits, JBJS 59 (6) (1977) 729–735.
[15] Y. Assouline-Dayan, C. Chang, A. Greenspan, Y. Shoenfeld, M.E. Gershwin, Pathogenesis and Natural History of Osteonecrosis, Seminars in Arthritis and Rheumatism, Elsevier, 2002, pp. 94–124.
[16] S.K. Das, A.K. Haldar, I. Ghosh, S.K. Saha, A. Das, S. Biswas, Serum magnesium and stable asthma: is there a link? Lung India: offic. Organ Indian Chest Soc. 27 (4) (2010) 205.
[17] R.K. Rude, H.E. Gruber, Magnesium deficiency and osteoporosis: animal and human observations, J. Nutr. Biochem. 15 (12) (2004) 710–716.
[18] Y. Rayssiguier, E. Gueux, D. Weiser, Effect of magnesium deficiency on lipid metabolism in rats fed a high carbohydrate diet, J. Nutr. 111 (11) (1981) 1876–1883.
[19] Y. Song, T.Y. Li, R.M. van Dam, J.E. Manson, F.B. Hu, Magnesium intake and plasma concentrations of markers of systemic inflammation and endothelial dysfunction in women–, Am. J. Clin. Nutr. 85 (4) (2007) 1068–1074.
[20] T. Ichiseki, T. Matsumoto, M. Nishino, A. Kaneuji, S. Katsuda, Oxidative stress and vascular permeability in steroid-induced osteonecrosis model, J. Orthop. Sci. 9 (5) (2004) 509–515.
[21] T. Ichiseki, A. Kaneuji, S. Katsuda, Y. Ueda, T. Sugimori, T. Matsumoto, DNA oxidation injury in bone early after steroid administration is involved in the pathogenesis of steroid-induced osteonecrosis, Rheumatology 44 (4) (2004) 456–460.
[22] M. Kuribayashi, M. Fujioka, K.A. Takahashi, Y. Arai, M. Ishida, T. Goto, T. Kubo, Vitamin E prevents steroid-induced osteonecrosis in rabbits, Acta Orthop. 81 (1) (2010) 154–160.
[23] P. Aghajanian, S. Hall, M.D. Wongworawat, S. Mohan, The roles and mechanisms of actions of vitamin C in bone: new developments, J. Bone Miner. Res. 30 (11) (2015) 1945–1955.
[24] G. Motomura, T. Yamamoto, K. Miyanishi, S. Jingushi, Y. Iwamoto, Combined effects of an anticoagulant and a lipid-lowering agent on the prevention of steroid-induced osteonecrosis in rabbits, Arthritis Rheum.: Offic. J. Am. Coll. Rheumatol. 50 (10) (2004) 3387–3391.
[25] L.-Z. Zheng, J.-L. Wang, L. Kong, L. Huang, L. Tian, Q.-Q. Pang, X.-L. Wang, L. Qin, Steroid-associated osteonecrosis animal model in rats, J. Orthopaed. Transl. 13 (2018) 13–24.
[26] J. Wang, F. Witte, T. Xi, Y. Zheng, K. Yang, Y. Yang, D. Zhao, J. Meng, Y. Li, W. Li, Recommendation for modifying current cytotoxicity testing standards for biodegradable magnesium-based materials, Acta Biomater. 21 (2015) 237–249.
[27] W.C. Liu, S. Chen, L. Zheng, L. Qin, Angiogenesis assays for the evaluation of angiogenic properties of orthopaedic biomaterials - a general review, Adv. Health. Mater. 6 (5) (2017).
[28] G. Carpentier, Contribution: angiogenesis analyzer, Imag. News 5 (2012).
[29] D. Zhu, Y. Su, B. Fu, H. Xu, Magnesium reduces blood-brain barrier permeability and regulates amyloid-beta transcytosis, Mol. Neurobiol. 55 (9) (2018) 7118–7131.
[30] I.o.L.A. Resources, Guide for the Care and Used of Laboratory Animals, National Academies Press, 1996.
[31] C. Kilkenny, W.J. Browne, I.C. Cuthill, M. Emerson, D.G. Altman, Improving bioscience research reporting: the ARRIVE guidelines for reporting animal research, PLoS Biol. 8 (6) (2010) e1000412.
[32] I.o.M.S.C.o.t.S.E.o.D.R. Intakes, Dietary Reference Intakes, Dietary Reference Intakes for Calcium, Phosphorus, Magnesium, Vitamin D, and Fluoride, National Academies Press (US), 1997.
[33] M. de Lourdes Lima, T. Cruz, J.C. Pousada, L.E. Rodrigues, K. Barbosa, V. Canguçu, The effect of magnesium supplementation in increasing doses on the control of type 2 diabetes, Diabetes Care 21 (5) (1998) 682–686.
[34] S. Chambial, S. Dwivedi, K.K. Shukla, P.J. John, P. Sharma, Vitamin C in disease prevention and cure: an overview, Indian J. Clin. Biochem. 28 (4) (2013) 314–328.
[35] G. Zhang, L. Qin, H. Sheng, K.W. Yeung, H.Y. Yeung, W.H. Cheung, J. Griffith, C.W. Chan, K.M. Lee, K.S. Leung, Epimedium-derived phytoestrogen exert beneficial effect on preventing steroid-associated osteonecrosis in rabbits with inhibition of both thrombosis and lipid-deposition, Bone 40 (3) (2007) 685–692.
[36] L. Qin, G. Zhang, H. Sheng, K.W. Yeung, H.Y. Yeung, C.W. Chan, W.H. Cheung, J. Griffith, K.H. Chiu, K.S. Leung, Multiple bioimaging modalities in evaluation of an experimental osteonecrosis induced by a combination of lipopolysaccharide and methylprednisolone, Bone 39 (4) (2006) 863–871.
[37] C.L. Duvall, W.R. Taylor, D. Weiss, R.E. Guldberg, Quantitative microcomputed tomography analysis of collateral vessel development after ischemic injury, Am. J. Physiol. Heart Circ. Physiol. 287 (1) (2004) H302–H310.
[38] G. Zhang, H. Sheng, Y.X. He, X.H. Xie, Y.X. Wang, K.M. Lee, K.W. Yeung, Z.R. Li, W. He, J.F. Griffith, K.S. Leung, L. Qin, Continuous occurrence of both insufficient neovascularization and elevated vascular permeability in rabbit proximal femur during inadequate repair of steroid-associated osteonecrotic lesions, Arthritis Rheum. 60 (10) (2009) 2966–2977.
[39] G.Q. Hou, C. Guo, G.H. Song, N. Fang, W.J. Fan, X.D. Chen, L. Yuan, Z.Q. Wang, Lipopolysaccharide (LPS) promotes osteoclast differentiation and activation by enhancing the MAPK pathway and COX-2 expression in RAW264.7 cells, Int. J. Mol. Med. 32 (2) (2013) 503–510.
[40] M.L. Bouxsein, S.K. Boyd, B.A. Christiansen, R.E. Guldberg, K.J. Jepsen, R. Muller, Guidelines for assessment of bone microstructure in rodents using micro-computed tomography, J. Bone Miner. Res. 25 (7) (2010) 1468–1486.
[41] D.H. Chow, L. Zheng, L. Tian, K.-S. Ho, L. Qin, X. Guo, Application of ultrasound accelerates the decalcification process of bone matrix without affecting histological and immunohistochemical analysis, J. Orthopaed. Transl. 17 (2019) 112–120.
[42] D.W. Dempster, J.E. Compston, M.K. Drezner, F.H. Glorieux, J.A. Kanis, H. Malluche, P.J. Meunier, S.M. Ott, R.R. Recker, A.M. Parfitt, Standardized nomenclature, symbols, and units for bone histomorphometry: a 2012 update of the report of the ASBMR Histomorphometry Nomenclature Committee, J. Bone Miner. Res. 28 (1) (2013) 2–17.
[43] U. Gröber, J. Schmidt, K. Kisters, Magnesium in prevention and therapy, Nutrients 7 (9) (2015) 8199–8226.
[44] R.K. Rude, H.E. Gruber, Magnesium deficiency and osteoporosis: animal and human observations, J. Nutr. Biochem. 15 (12) (2004) 710–716.
[45] G. Rolla, C. Bucca, M. Bugiani, A. Oliva, L. Branciforte, Hypomagnesemia in chronic obstructive lung disease: effect of therapy, Magnes. Trace. Elem. 9 (3) (1990) 132–136.
[46] J.J. DiNicolantonio, J.H. O'Keefe, W. Wilson, Subclinical magnesium deficiency: a principal driver of cardiovascular disease and a public health crisis, Open Heart 5 (1) (2018) e000668.
[47] E. of Ekenstam, G. Stålenheim, R. Hällgren, The acute effect of high dose corticosteroid treatment on serum osteocalcin, Metabolism 37 (2) (1988) 141–144.
[48] I. Kanazawa, T. Yamaguchi, Y. Tada, M. Yamauchi, S. Yano, T. Sugimoto, Serum osteocalcin level is positively associated with insulin sensitivity and secretion in patients with type 2 diabetes, Bone 48 (4) (2011) 720–725.
[49] J.L. Nadler, T. Buchanan, R. Natarajan, I. Antonipillai, R. Bergman, R. Rude, Magnesium deficiency produces insulin resistance and increased thromboxane synthesis, Hypertension 21 (6_pt_2) (1993) 1024–1029.
[50] L.M.M. Gommers, J.G.J. Hoenderop, R.J.M. Bindels, J.H.F. de Baaij, Hypomagnesemia in type 2 diabetes: a vicious circle? Diabetes 65 (1) (2016) 3–13.
[51] F.P. Cantatore, E. Crivellato, B. Nico, D. Ribatti, Osteocalcin is angiogenic in vivo, Cell Biol. Int. 29 (7) (2005) 583–585.

[52] M.B. Kahn, N.Y. Yuldasheva, R.M. Cubbon, J. Smith, S.T. Rashid, H. Viswambharan, H. Imrie, A. Abbas, A. Rajwani, A. Aziz, Insulin resistance impairs circulating angiogenic progenitor cell function and delays endothelial regeneration, Diabetes 60 (4) (2011) 1295–1303.
[53] I. Juhan-Vague, M. Alessi, PAI-1, obesity, insulin resistance and risk of cardiovascular events, Thromb. Haemostasis 78 (1) (1997) 656–660.
[54] I. Juhan-Vague, M.C. Alessi, P.E. Morange, Hypofibrinolysis and increased PAI-1 are linked to atherothrombosis via insulin resistance and obesity, Ann. Med. 32 (2000) 78–84.
[55] F. Guerrero-Romero, M. Rodriguez-Moran, Serum magnesium in the metabolically-obese normal-weight and healthy-obese subjects, Eur. J. Intern. Med. 24 (7) (2013) 639–643.
[56] F. Guerrero-Romero, H. Tamez-Perez, G.e. González-González, A. Salinas-Martinez, J. Montes-Villarreal, J. Trevino-Ortiz, M. Rodriguez-Moran, Oral magnesium supplementation improves insulin sensitivity in non-diabetic subjects with insulin resistance. A double-blind placebo-controlled randomized trial, Diabetes Metabol. 30 (3) (2004) 253–258.
[57] S. Okazaki, S. Nagoya, H. Matsumoto, K. Mizuo, J. Shimizu, S. Watanabe, H. Inoue, T. Yamashita, TLR4 stimulation and corticosteroid interactively induce osteonecrosis of the femoral head in rat, J. Orthop. Res. 34 (2) (2016) 342–345.
[58] T. Irisa, T. Yamamoto, K. Miyanishi, A. Yamashita, Y. Iwamoto, Y. Sugioka, K. Sueishi, Osteonecrosis induced by a single administration of low-dose lipopolysaccharide in rabbits, Bone 28 (6) (2001) 641–649.
[59] H.J. Freeman, W.P. Kwan, Non-corticosteroid-associated osteonecrosis of the femoral heads in two patients with inflammatory bowel disease, N. Engl. J. Med. 329 (18) (1993) 1314–1316.
[60] F.H. Nielsen, Magnesium, inflammation, and obesity in chronic disease, Nutr. Rev. 68 (6) (2010) 333–340.
[61] Y. Rayssiguier, P. Libako, W. Nowacki, E. Rock, Magnesium deficiency and metabolic syndrome: stress and inflammation may reflect calcium activation, Magnes. Res. 23 (2) (2010) 73–80.
[62] L. Ginaldi, M.C. Di Benedetto, M. De Martinis, Osteoporosis, inflammation and ageing, Immun. Ageing 2 (1) (2005) 14.
[63] N.J. Abbott, Inflammatory mediators and modulation of blood–brain barrier permeability, Cell. Mol. Neurobiol. 20 (2) (2000) 131–147.
[64] S. Islam, F. Hassan, G. Tumurkhuu, J. Dagvadorj, N. Koide, Y. Naiki, I. Mori, T. Yoshida, T. Yokochi, Bacterial lipopolysaccharide induces osteoclast formation in RAW 264.7 macrophage cells, Biochem. Biophys. Res. Commun. 360 (2) (2007) 346–351.
[65] M.S. Schappe, K. Szteyn, M.E. Stremska, S.K. Mendu, T.K. Downs, P.V. Seegren, M.A. Mahoney, S. Dixit, J.K. Krupa, E.J. Stipes, Chanzyme TRPM7 mediates the Ca2+ influx essential for lipopolysaccharide-induced toll-like receptor 4 endocytosis and macrophage activation, Immunity 48 (1) (2018) 59–74 e5.
[66] M. Tauseef, N. Knezevic, K.R. Chava, M. Smith, S. Sukriti, N. Gianaris, A.G. Obukhov, S.M. Vogel, D.E. Schraufnagel, A. Dietrich, TLR4 activation of TRPC6-dependent calcium signaling mediates endotoxin-induced lung vascular permeability and inflammation, J. Exp. Med. 209 (11) (2012) 1953–1968.
[67] H. Kajiya, Calcium signaling in osteoclast differentiation and bone resorption, in: M.S. Islam (Ed.), Calcium Signaling, Springer Netherlands, Dordrecht, 2012, pp. 917–932.
[68] E.M. Grössinger, M. Kang, L. Bouchareychas, R. Sarin, D.R. Haudenschild, L.N. Borodinsky, I.E. Adamopoulos, Ca2+-Dependent regulation of NFATc1 via KCa3. 1 in inflammatory osteoclastogenesis, J. Immunol. 200 (2) (2018) 749–757.
[69] M. Nauck, G. Karakiulakis, A.P. Perruchoud, E. Papakonstantinou, M. Roth, Corticosteroids inhibit the expression of the vascular endothelial growth factor gene in human vascular smooth muscle cells, Eur. J. Pharmacol. 341 (2–3) (1998) 309–315.
[70] M.F. Ryan, The role of magnesium in clinical biochemistry: an overview, Ann. Clin. Biochem. 28 (1) (1991) 19–26.
[71] J. Tonkin, L. Temmerman, R.D. Sampson, E. Gallego-Colon, L. Barberi, D. Bilbao, M.D. Schneider, A. Musarò, N. Rosenthal, Monocyte/macrophage-derived IGF-1 orchestrates murine skeletal muscle regeneration and modulates autocrine polarization, Mol. Ther. 23 (7) (2015) 1189–1200.
[72] J.-P. Bonjour, M. Schüren, T. Chevalley, P. Ammann, R. Rizzoli, Protein intake, IGF-1 and osteoporosis, Osteoporos. Int. 7 (3) (1997) 36–42.
[73] M.A. Bredella, M. Torriani, R.H. Ghomi, B.J. Thomas, D.J. Brick, A.V. Gerweck, C.J. Rosen, A. Klibanski, K.K. Miller, Vertebral bone marrow fat is positively associated with visceral fat and inversely associated with IGF-1 in obese women, Obesity 19 (1) (2011) 49–53.
[74] M. Maggio, F. De Vita, F. Lauretani, V. Buttò, G. Bondi, C. Cattabiani, A. Nouvenne, T. Meschi, E. Dall'Aglio, G. Ceda, IGF-1, the cross road of the nutritional, inflammatory and hormonal pathways to frailty, Nutrients 5 (10) (2013) 4184–4205.
[75] A.R. Guntur, C.J. Rosen, IGF-1 regulation of key signaling pathways in bone, BoneKEy Rep. 2 (2013).
[76] S. Shigematsu, K. Yamauchi, K. Nakajima, S. Iijima, T. Aizawa, K. Hashizume, IGF-1 regulates migration and angiogenesis of human endothelial cells, Endocr. J. 46 (Suppl) (1999) S59–S62.
[77] M. Maggio, G. Ceda, F. Lauretani, C. Cattabiani, E. Avantaggiato, S. Morganti, F. Ablondi, S. Bandinelli, L. Dominguez, M. Barbagallo, Magnesium and anabolic hormones in older men, Int. J. Androl. 34 (6pt2) (2011) e594–e600.
[78] I. Dørup, A. Flyvbjerg, M.E. Everts, T. Clausen, Role of insulin-like growth factor-1 and growth hormone in growth inhibition induced by magnesium and zinc deficiencies, Br. J. Nutr. 66 (3) (1991) 505–521.
[79] S. Boonrungsiman, E. Gentleman, R. Carzaniga, N.D. Evans, D.W. McComb, A.E. Porter, M.M. Stevens, The role of intracellular calcium phosphate in osteoblast-mediated bone apatite formation, Proc. Natl. Acad. Sci. Unit. States Am. 109 (35) (2012) 14170–14175.
[80] K.H. Baek, K.W. Oh, W.Y. Lee, S.S. Lee, M.K. Kim, H.S. Kwon, E.J. Rhee, J.H. Han, K.H. Song, B.Y. Cha, Association of oxidative stress with postmenopausal osteoporosis and the effects of hydrogen peroxide on osteoclast formation in human bone marrow cell cultures, Calcif. Tissue Int. 87 (3) (2010) 226–235.
[81] W.J. Boyle, W.S. Simonet, D.L. Lacey, Osteoclast differentiation and activation, Nature 423 (6937) (2003) 337.
[82] L.Z. Zheng, H.J. Cao, S.H. Chen, T. Tang, W.M. Fu, L. Huang, D.H. Chow, Y.X. Wang, J.F. Griffith, W. He, H. Zhou, W. Zhao, G. Zhang, X.L. Wang, L. Qin, Blockage of src by specific siRNA as a novel therapeutic strategy to prevent destructive repair in steroid-associated osteonecrosis in rabbits, J. Bone Miner. Res. (2015).
[83] F.I. Wolf, V. Trapani, M. Simonacci, S. Ferré, J.A. Maier, Magnesium deficiency and endothelial dysfunction: is oxidative stress involved? Magnes. Res. 21 (1) (2008) 58–64.
[84] S.J. Padayatty, A. Katz, Y. Wang, P. Eck, O. Kwon, J.-H. Lee, S. Chen, C. Corpe, A. Dutta, S.K. Dutta, Vitamin C as an antioxidant: evaluation of its role in disease prevention, J. Am. Coll. Nutr. 22 (1) (2003) 18–35.
[85] N.E. Lane, Therapy insight: osteoporosis and osteonecrosis in systemic lupus erythematosus, Nat. Rev. Rheumatol. 2 (10) (2006) 562.
[86] M. El Assar, J. Angulo, L. Rodríguez-Mañas, Oxidative stress and vascular inflammation in aging, Free Radic. Biol. Med. 65 (2013) 380–401.
[87] R. Gill, A. Tsung, T. Billiar, Linking oxidative stress to inflammation: toll-like receptors, Free Radic. Biol. Med. 48 (9) (2010) 1121–1132.
[88] S. Bryan, B. Baregzay, D. Spicer, P.K. Singal, N. Khaper, Redox-inflammatory synergy in the metabolic syndrome, Can. J. Physiol. Pharmacol. 91 (1) (2013) 22–30.
[89] K.-J. Kim, S. Choi, Y. Sang Cho, S.-J. Yang, Y.-S. Cho, K.K. Kim, Magnesium ions enhance infiltration of osteoblasts in scaffolds via increasing cell motility, J. Mater. Sci. Mater. Med. 28 (6) (2017) 96.
[90] H. Yao, J. Xu, N. Zheng, J. Wang, S. Mok, Y. Lee, L. Shi, J. Wang, J. Yue, S. Yung, Intra-articular Injection of Magnesium Chloride Attenuates Osteoarthritis Progression in Rats, Osteoarthritis and Cartilage, (2019).
[91] C.-H. Lee, Z. Wen, Y. Chang, S. Huang, C. Tang, W. Chen, S. Hsieh, C. Hsieh, Y. Jean, Intra-articular magnesium sulfate (MgSO4) reduces experimental osteoarthritis and nociception: association with attenuation of N-methyl-D-aspartate (NMDA) receptor subunit 1 phosphorylation and apoptosis in rat chondrocytes, Osteoarthritis Cartilage 17 (11) (2009) 1485–1493.
[92] I. Slutsky, N. Abumaria, L.-J. Wu, C. Huang, L. Zhang, B. Li, X. Zhao, A. Govindarajan, M.-G. Zhao, M. Zhuo, Enhancement of learning and memory by elevating brain magnesium, Neuron 65 (2) (2010) 165–177.
[93] Y. Lai, Y. Li, H. Cao, J. Long, X. Wang, L. Li, C. Li, Q. Jia, B. Teng, T. Tang, Osteogenic magnesium incorporated into PLGA/TCP porous scaffold by 3D printing for repairing challenging bone defect, Biomaterials 197 (2019) 207–219.
[94] F.G.-C. Bachiller, A.P. Caballer, L.F. Portal, Avascular necrosis of the femoral head after femoral neck fracture, Clin. Orthop. Relat. Res. 399 (2002) 87–109.
[95] Y. Zhang, J. Xu, Y.C. Ruan, M.K. Yu, M. O'Laughlin, H. Wise, D. Chen, L. Tian, D. Shi, J. Wang, S. Chen, J.Q. Feng, D.H. Chow, X. Xie, L. Zheng, L. Huang, S. Huang, K. Leung, N. Lu, L. Zhao, H. Li, D. Zhao, X. Guo, K. Chan, F. Witte, H.C. Chan, Y. Zheng, L. Qin, Implant-derived magnesium induces local neuronal production of CGRP to improve bone-fracture healing in rats, Nat. Med. 22 (10) (2016) 1160–1169.